Advances in global bioavailable strontium isoscapes

- 2 Clement P. Bataille^{1*}, Brooke E. Crowley^{2,3}, Matthew J. Wooller^{4,5}, Gabriel J. Bowen⁶
- ¹Department of Earth and Environmental Sciences, University of Ottawa, 120 University, Ottawa, ON
- 4 Canada, K1N 6N5. cbataill@uottawa.ca
- 5 ² Department of Geology, University of Cincinnati, 500 Geology Physics Building, 345 Clifton Court,
- 6 Cincinnati, Ohio, 45221-0013, USA. crowlebk@UCMAIL.UC.EDU
- 7 Department of Anthropology, University of Cincinnati, 481 Braunstein Hall, Cincinnati, Ohio,
- 8 45221-0380, USA

1

- 9 ⁴ Alaska Stable Isotope Facility, Water and Environmental Research Center, Institute of Northern
- 10 Engineering, University of Alaska Fairbanks, Fairbanks, Alaska, 99775 USA. mjwooller@alaska.edu
- ⁵ Marine Biology Department, College of Fisheries and Ocean Sciences, University of Alaska
- 12 Fairbanks, Fairbanks, Alaska, 99775 USA
- 13 ⁶ Department of Geology & Geophysics and Global Change & Sustainability Center, University of
- Utah, 115 S 1460 E, Salt Lake City, UT 84112, USA. gabe.bowen@utah.edu
- * Correspondence and requests for materials should be addressed to C.P.B. (email:
- 16 cbataill@uottawa.ca)

Abstract

17

- Strontium isotope ratios (87Sr/86Sr) are a popular tool in provenance applications in
- archeology, forensics, paleoecology, and environmental sciences. Using bioavailable ⁸⁷Sr/⁸⁶Sr
- 20 in provenance studies requires comparing the ⁸⁷Sr/⁸⁶Sr of a sample of interest to that of
- 21 ⁸⁷Sr/⁸⁶Sr baselines. Historically, these baselines required building empirical datasets from
- 22 plants or local animals to characterize the ⁸⁷Sr/⁸⁶Sr available to local ecosystems (bioavailable
- ⁸⁷Sr/⁸⁶Sr). However, researchers are increasingly relying on modeled bioavailable ⁸⁷Sr/⁸⁶Sr
- 24 maps (called isoscapes). We review the advantages and limitations of existing approaches to
- 25 mapping bioavailable ⁸⁷Sr/⁸⁶Sr for provenance studies and propose a globally applicable,
- scalable, and editable framework for creating bioavailable ⁸⁷Sr/⁸⁶Sr isoscapes. This
- framework relies on: 1) Compiling global bioavailable ⁸⁷Sr/⁸⁶Sr data; 2) Mapping ⁸⁷Sr/⁸⁶Sr
- variability in rocks; 3) Leveraging global environmental covariates; and 4) Applying a
- 29 random forest regression method that integrates these data to predict bioavailable ⁸⁷Sr/⁸⁶Sr.
- When the random-forest model is applied at the global scale it performs well (explaining 60%
- of the variance of the global bioavailable ⁸⁷Sr/⁸⁶Sr dataset), and accounts for geological,
- 32 geomorphological and atmospheric controls. In data-rich regions (e.g., Europe), the global
- bioavailable ⁸⁷Sr/⁸⁶Sr isoscape can be successfully extrapolated to broad regions without
- bioavailable ⁸⁷Sr/⁸⁶Sr data. However, we also show that this extrapolation may not be valid in
- exceptionally geologically complex and data-poor regions (e.g., Madagascar). We suggest
- research directions to improve the accuracy of global bioavailable ⁸⁷Sr/⁸⁶Sr isoscapes, which
- include: 1) Increasing the collection of bioavailable datasets in data-poor regions; 2)
- Harmonizing data management practices and metadata collection for bioavailable ⁸⁷Sr/⁸⁶Sr
- data; and 3) Relying on advances in remote sensing and geological mapping techniques to
- 40 improve geological covariates. While significant potential to refine ⁸⁷Sr/⁸⁶Sr isoscapes
- remains, the data products provided in this review form a basis for using ⁸⁷Sr/⁸⁶Sr data in
- 42 large-scale provenance studies, opening new research avenues in a range of fields.

Keywords: Provenance, Random Forest, Regression, Madagascar, Migration, Isotopes;

1. Introduction

43

44

45

46

47 48

49

50 51

52

53

54

55

56

57

58

59

60

61

62

63

64

65

66

67

68

69

70

71

72

73

74

75

76

77

78 79

80

81 82

83 84

85

86

87

Strontium (Sr) isotope ratios (87Sr/86Sr) display a unique and predictable patterns of variability on the Earth's surface that follow the geological age and lithology of bedrocks (Bataille and Bowen, 2012). As rocks interact with the hydrosphere, atmosphere and biosphere, bedrock Sr is transferred to other reservoirs on the Earth's surface, such as soils and plants. Geologists have long recognized and capitalized on this natural ⁸⁷Sr/⁸⁶Sr variability to trace the provenance of geological materials (Reviewed in Banner, 2004; Capo et al., 1998b; Peucker-Ehrenbrink and Fiske, 2019). In the last few decades, researchers have also recognized the potential for ⁸⁷Sr/⁸⁶Sr data to solve new questions in ecology, paleoecology, and archeology (Reviewed in Åberg, 1995; Bentley, 2006; Crowley et al., 2017a; Hobson et al., 2010; Makarewicz and Sealy, 2015). This uptick of interest in ⁸⁷Sr/⁸⁶Sr geochemistry has coincided with analytical advances and the development of multi-collector inductively coupled plasma mass spectrometers (MC-ICPMS). This instrumentation and its greater global availability has made ⁸⁷Sr/⁸⁶Sr analysis more mainstream by accelerating throughput and enhancing cost-effectiveness while also facilitating the development of new applications in the life sciences such as laser ablation of incrementally growing tissues (e.g., fin rays and otoliths; Brennan et al., 2015b; Willmes et al., 2016). With these advances, ⁸⁷Sr/⁸⁶Sr geochemistry has become a critical tool for tracing the mobility and/or geographic origin of biological material in ecology (Reviewed in Hobson et al., 2010), paleoecology (Reviewed in Crowley et al., 2017a), archeology (Reviewed in Bentley, 2006), forensic sciences (Reviewed in Makarewicz and Sealy, 2015), and food sciences (Reviewed in Coelho et al., 2017). All of these applications rely on comparing the ⁸⁷Sr/⁸⁶Sr of a given substrate with the isotopic signatures of its potential sources. To facilitate the interpretation of ⁸⁷Sr/⁸⁶Sr data in these applications, it is critical to constrain the spatial variability of ⁸⁷Sr/⁸⁶Sr in the geosphere, hydrosphere and biosphere.

Isoscapes are spatially explicit predictions of isotopic variations. These predictions can be produced either through geostatistical interpolation of observed isotopic data, or through mechanistic model based on first principles of isotope geochemistry (Bowen and West, 2008). Over the last few decades, isoscapes of hydrogen, carbon, oxygen, and nitrogen have been developed, building upon the growing number of isotopic observations (Bowen and Wilkinson, 2002; Still and Powell, 2010; West et al., 2010a). These isoscapes have become a routine tool to understand movement patterns of animals and humans and environmental and biological processes (West et al., 2010b). Isoscape science has recently contributed to research on many high-profile science questions, from partitioning the global hydrological cycle (Good et al., 2015) to assessing the population dynamics of critical species (Brennan et al., 2019). As such, the field of isotope provenancing is rapidly expanding and entering the realm of data science, for example through large initiatives to integrate relevant data in centralized repositories (Pauli et al., 2017), and community efforts to make modeling products widely accessible (Bowen et al., 2014). Historically, interest in, and development of, Sr isoscapes has lagged hydrogen, oxygen or carbon isotopic systems. The primary reasons are that ⁸⁷Sr/⁸⁶Sr analysis is challenging, relatively expensive, and relies on instrumentation that is not as widely available as that needed for conducting light stable isotope analyses. However, ⁸⁷Sr/⁸⁶Sr analyses have progressively emerged as a powerful complementary tool in provenance studies due to their unique spatial patterns of isotopic variability, with pioneering work having been conducted in archeology (Ezzo et al., 1997; Price et al., 1994; Sillen et al., 1998), paleoecology (Hoppe et al., 1999), ecology (Chamberlain et al., 1997; Kennedy et al., 2002, 2000; Koch et al., 1995b, 1995a; Thorrold and Shuttleworth, 2000), and ecosystem dynamics (Blum et al., 2000; Gosz et al., 1983). In the last decade, the development and application of ⁸⁷Sr/⁸⁶Sr isoscapes has grown exponentially, driven by high-profile applications in archeology (e.g., Copeland et al., 2011), paleoecology (e.g., Price et al., 2017), ecology (e.g., Brennan et al., 2019; Glassburn et al., 2018), and forensic science (e.g., Bartelink and Chesson, 2019; Kramer et al., 2020).

This review synthesizes the current state of the rapidly evolving and interdisciplinary research associated with ⁸⁷Sr/⁸⁶Sr isoscapes. We begin by reviewing spatial ⁸⁷Sr/⁸⁶Sr trends on the Earth surface with a focus on large-scale patterns derived from the interactions of the geosphere, hydrosphere, atmosphere and biosphere. We then compare different approaches for making ⁸⁷Sr/⁸⁶Sr isoscapes in terrestrial and freshwater environments. In an effort to better integrate interdisciplinary ⁸⁷Sr/⁸⁶Sr data, we present the first global compilation of ⁸⁷Sr/⁸⁶Sr data from different environmental substrates. We use this compilation to produce a global model for predicting bioavailable ⁸⁷Sr/⁸⁶Sr and demonstrate the potential of using this approach to generate ⁸⁷Sr/⁸⁶Sr isoscapes at the regional scale in two regions: Europe and Madagascar. We conclude by discussing key knowledge gaps and new research avenues opened by this global data science approach.

2. Strontium isotope cycling

2.1 Strontium isotopes geochemistry

Strontium is a divalent alkaline earth trace element with four naturally occurring isotopes: 84 Sr (\sim 0.56%), 86 Sr (\sim 9.87%), 87 Sr (\sim 7.04%) and 88 Sr (\sim 82.53%). 84 Sr, 86 Sr, 87 Sr and 88 Sr are all stable isotopes (i.e., do not radioactively decay). Unlike the other Sr isotopes, 87 Sr is the radiogenic daughter product of rubidium 87 (87 Rb; decay constant $\lambda = 1.42 \times 10-11$ year⁻¹; Steiger and Jäger, 1977). The ratio of 87 Sr to the other isotopes is therefore a function of the variable abundance of 87 Sr. In provenance studies, Sr isotope variations are typically represented using the ratio of 87 Sr relative to 86 Sr after correction for any mass-dependent fractionation by normalization to a fixed 86 Sr/ 88 Sr (0.1194; Nier, 1938). The resulting 87 Sr/ 86 Sr is thus not a function of isotopic fractionation processes but only reflects the mixing of isotopically distinct Sr sources.

2.2 Strontium isotopes in the geosphere

The ⁸⁷Sr/⁸⁶Sr in modern rocks and minerals is both mineral-dependent (initial ⁸⁷Rb, ⁸⁷Sr, and ⁸⁶Sr abundance), and time-dependent (radioactive decay of ⁸⁷Rb to ⁸⁷Sr). At the time of our planet's formation, the bulk Earth reservoir had a relatively homogeneous ⁸⁷Sr/⁸⁶Sr signature of around 0.699 (Wetherill et al., 1973). As geochemical differentiation progressed, Sr and Rb concentrated in melts that preferentially contributed to oceanic and continental crusts. This partitioning resulted in increased ⁸⁷Rb/⁸⁶Sr in the continental crust relative to the oceanic crust and the residual mantle (Faure and Powell, 1972), and over time, this led to differences in ⁸⁷Sr/⁸⁶Sr among geologic pools with the progressive decay of ⁸⁷Rb into ⁸⁷Sr.

These combined effects of geochemical partitioning of Rb and Sr and radioactive decay explain the large range of ⁸⁷Sr/⁸⁶Sr in igneous, sedimentary, and metamorphic rocks. With equal initial ⁸⁷Rb/⁸⁶Sr, older igneous rocks have higher ⁸⁷Sr/⁸⁶Sr than younger rocks because ⁸⁷Rb has had more time to decay in the older reservoir. At equal age, more felsic

rocks (with higher ⁸⁷Rb/⁸⁶Sr) have higher ⁸⁷Sr/⁸⁶Sr than mafic rocks (with lower ⁸⁷Rb/⁸⁶Sr) because more ⁸⁷Rb is available to decay into ⁸⁷Sr. Old felsic igneous rock units (e.g., cratonic shields) have the highest measured ⁸⁷Sr/⁸⁶Sr (>0.720), while newly formed mafic igneous rock units (e.g., basalts, volcanic arcs) have the lowest ⁸⁷Sr/⁸⁶Sr (~0.703) (Peucker-Ehrenbrink and Fiske, 2019).

Siliciclastic sediments inherit ⁸⁷Sr/⁸⁶Sr from their parent rocks but are usually composed of a mixture of minerals with distinct parent rock, and thus different isotopic ratios. Because local bedrock sources dominate the ⁸⁷Sr/⁸⁶Sr, recently deposited siliciclastic sediments from young igneous rocks (e.g., volcanic arcs) tend to have lower ⁸⁷Sr/⁸⁶Sr than those forming in older felsic environments (Bataille et al., 2014). However, it becomes challenging to assess the original parent rock for older sediments due to tectonic and geomorphological evolution of the surface. As sediments are exposed and reworked on the surface, the preferential removal of Sr relative to Rb in weathering and metamorphic processes can subsequently modify their ⁸⁷Sr/⁸⁶Sr leading to additional ⁸⁷Sr/⁸⁶Sr variability in older sedimentary units (Bataille et al., 2014). Carbonate rocks, on the other hand, primarily inherit their ⁸⁷Sr/⁸⁶Sr from seawater (the exceptions being metamorphic, igneous or soil carbonates). They have a narrow range in ⁸⁷Sr/⁸⁶Sr because 1) seawater ⁸⁷Sr/⁸⁶Sr has remained within a tight range throughout the Phanerozoic (0.707 and 0.709; McArthur et al., 2001), and 2) carbonates have small amounts of Rb but large amounts of Sr (Sr readily substitutes for calcium), which means their ⁸⁷Sr/⁸⁶Sr does not evolve significantly through time.

Metamorphism can alter the ⁸⁷Sr/⁸⁶Sr of igneous and sedimentary rock units, which can lead to highly variable ⁸⁷Sr/⁸⁶Sr in metamorphic rocks. For example, metalimestones in the Himalayas have much higher ⁸⁷Sr/⁸⁶Sr than non-metamorphosed marine carbonates due to exchange of ⁸⁷Sr between silicates and carbonates during metamorphism (Bickle et al., 2001). Similarly, hydrothermal metamorphism can homogenize the ⁸⁷Sr/⁸⁶Sr of lithologically distinct sedimentary rock units (Bickle et al., 1988). Ultimately, the combination of igneous, sedimentary and metamorphic processes leads to considerable variability of ⁸⁷Sr/⁸⁶Sr in the geosphere. Bedrock ⁸⁷Sr/⁸⁶Sr ranges from 0.702 in ophiolites to more than 1 in old felsic Archean rocks (Faure and Powell, 1972). The ⁸⁷Sr/⁸⁶Sr distribution in rocks is positively skewed with average upper crust ⁸⁷Sr/⁸⁶Sr around 0.716.

2.3 Strontium isotopes in soils and plants

Soils primarily inherit their ⁸⁷Sr/⁸⁶Sr composition from parent rock, and consequently ⁸⁷Sr/⁸⁶Sr patterns in soils follow those of the underlying geology (Fig. 1). However, the observed relationship between soil and local bedrock ⁸⁷Sr/⁸⁶Sr is rarely 1:1. This is because soil ⁸⁷Sr/⁸⁶Sr is buffered by the influence of additional sources of Sr with distinct ⁸⁷Sr/⁸⁶Sr compositions (Fig. 1). For example, unconsolidated sediments, such as fluvial terraces and glacial till or loess, typically have different ⁸⁷Sr/⁸⁶Sr than the underlying bedrock (Börker et al., 2018). In the Midwestern USA, glacial till coming from the Canadian craton covers much of the bedrock and is the dominant source of Sr to soils (Hedman et al., 2009; Widga et al., 2017). Downwind of desert zones, dust often recharges soil primary minerals and can even serve as the dominant parent material in some cases (Aarons et al., 2017; Frumkin and Stein, 2004; Grousset et al., 1992; Miller et al., 2014; Naiman et al., 2000; Widory et al., 2010). Tephra deposition near volcanic centers can also provide easily weatherable and Sr-rich primary minerals to soils and ecosystems that will dominate over bedrock sources (Chadwick et al., 2009). Last but not least, near the coast, sea salt aerosol deposition can influence the exchangeable Sr fraction of soil (Hartman and Richards, 2014; Quade et al., 1995; Whipkey et al., 2000).

Different soil fractions can also have distinct ⁸⁷Sr/⁸⁶Sr compositions due to differential weathering and soil mixing processes (Fig. 1). In particular, the ⁸⁷Sr/⁸⁶Sr ratio of the soil exchangeable Sr fraction (defined as the fraction that is extractable using ammonium nitrate leaching from a top soil sample) can differ considerably from the bulk digested soil mineral fraction or from soil samples collected at different depths (Gryschko et al., 2005; Poszwa et al., 2004). The soil exchangeable Sr corresponds primarily to Sr dissolved in soil water and available to plants but also includes some Sr weakly absorbed on clays (Capo et al., 1998). The ⁸⁷Sr/⁸⁶Sr of this soil exchangeable Sr is strongly influenced by soil age. In a young soil, Sr-rich and rapidly weathering primary minerals (e.g., carbonates, plagioclases) will be the dominant contributors to the exchangeable Sr pool (Chadwick et al., 2009; Vitousek et al., 1999). However, as a soil matures, these rapidly weathering minerals can be exhausted and other primary minerals with distinct ⁸⁷Sr/⁸⁶Sr will dominate the Sr budget. As soils become more and more weathered, fewer primary minerals are available, and other sources (e.g., dust and other aerosols) increasingly contribute to the exchangeable Sr budget (Chadwick et al., 2009; Vitousek et al., 1999). The contribution of these atmospheric sources to the dissolved soil ⁸⁷Sr/⁸⁶Sr budget will depend in the rate of deposition, weatherability, Sr content, and ⁸⁷Sr/⁸⁶Sr (Pett-Ridge et al., 2009). In some cases, atmospheric deposition will dominate over bedrock sources even when soils are young (Miller et al., 2014), whereas in other cases, bedrock remains the dominant Sr source even when soils are highly weathered (Bern et al., 2005; Porder et al., 2006).

Plants take up Sr from the exchangeable soil fraction (Fig. 1). However, differences between ⁸⁷Sr/⁸⁶Sr in plants and the exchangeable Sr fraction can occur, particularly in regions where multiple sources of Sr mix into soils (e.g., atmospheric vs. parent rock Sr; Hartman and Richards, 2014; Laffoon et al., 2012; Snoeck et al., 2016). As mentioned above, differential weathering and soil mixing processes can lead to variable ⁸⁷Sr/⁸⁶Sr along the soil profile (Reynolds et al., 2012). This variability is propagated among plants with different rooting depth (Poszwa et al., 2004).

2.4 Strontium isotopes in surface waters

180

181

182

183

184

185

186

187

188

189

190

191

192

193

194

195

196

197

198

199

200

201

202

203

204

205

206

207

208

209

210

211

212

213

214

215

216

217

218

219

220221

222

223

224

Water inherits ⁸⁷Sr/⁸⁶Sr from rock weathering (Fig. 1). Consequently, spatial patterning of ⁸⁷Sr/⁸⁶Sr in the hydrosphere reflects that of rocks exposed on the surface and in aguifers, with high ⁸⁷Sr/⁸⁶Sr in rivers draining cratons and low ⁸⁷Sr/⁸⁶Sr in rivers draining mafic rock units (Peucker-Ehrenbrink and Fiske, 2019). However, the contributions of different minerals and rock units to the dissolved Sr pool vary broadly based on their weathering rate and Sr content, which in turn leads to distinct ⁸⁷Sr/⁸⁶Sr between the hydrosphere and geosphere (Blum et al., 1993). During igneous rock weathering, plagioclases contribute more than radiogenic minerals to the dissolved Sr flux due to their higher Sr content and weathering rate (Bain and Bacon, 1994; Clow et al., 1997; Pett-Ridge et al., 2009). Similarly Sr-rich and easily weatherable carbonates and evaporites contribute disproportionately to the dissolved Sr in the hydrosphere (Peucker-Ehrenbrink and Fiske, 2019). Even trace amounts of calcite in silicates can dominate the entire Sr budget in large rivers (Clow et al., 1997). At the scale of a catchment, the flux of Sr from isotopically distinct rock units is also modulated by geomorphological, climatic and environmental conditions (Bataille et al., 2014). For example, sediments from mountainous zones will contribute disproportionately to the total Sr flux and strongly influence the ⁸⁷Sr/⁸⁶Sr as they weathered along the entire course of a river (Galy and France-Lanord, 1999) and its floodplains (Bickle et al., 2018; Lupker et al., 2012).

Allochthonous surface sediments, such as glacial till, may also impact river ⁸⁷Sr/⁸⁶Sr (Curtis and Stueber, 1973). In boreal and arctic regions, seasonal land cover changes (i.e., vegetation, ice cover) can lead to strong seasonal ⁸⁷Sr/⁸⁶Sr fluctuations because of variable contribution of rock units within a catchment (Douglas et al., 2013; Voss et al., 2014). Ultimately, spatial ⁸⁷Sr/⁸⁶Sr trends in the hydrosphere follow those of the geosphere but with lower ratios and variability due to the buffering effect of carbonate weathering (Palmer and Edmond, 1992).

2.5 Strontium isotopes in animal tissues

Primary terrestrial consumers obtain the majority of their Sr from diet (Fig. 1; Glorennec et al., 2016). As plants are at the base of many terrestrial food chains, ⁸⁷Sr/⁸⁶Sr for animals usually reflects that of local plants (Willmes et al., 2014). However, drinking water can contribute significantly to the Sr inputs when (1) water is Sr-rich (e.g., carbonate landscapes), or (2) animals drink frequently (Lewis et al., 2017). Different taxa sample Sr differently on the landscape depending on their feeding habits and feeding ranges (Lengfelder et al., 2019). For example, at a given location, small herbivores with a local feeding range (e.g., rodents) often have distinct ⁸⁷Sr/⁸⁶Sr signatures from larger herbivores (e.g., deer) because the larger animals integrate Sr sources over a larger area (Feranec et al., 2007; Lengfelder et al., 2019). Aquatic animals (e.g., tapirs) may also have distinct ⁸⁷Sr/⁸⁶Sr if they feed on riparian or freshwater foods (e.g., Hedman et al., 2009; Wallace et al., 2019). There are more challenges associated with predicting how different environmental sources contribute to consumer Sr with an increase in the complexity of animal feeding behaviors (e.g., large migratory herbivores, omnivores and carnivores) (Hoppe et al., 1999). At the extreme, humans can eat local terrestrial resources, hunt migratory mammals, harvest marine resources, inheriting a potentially very complex mixture of ⁸⁷Sr/⁸⁶Sr sources (Fig. 1; Bentley, 2006). Humans can also obtain resources from distant localities via trade (reviewed in Bentley, 2006).

Sr is integrated over variable timescales in different animal tissues (Makarewicz and Sealy, 2015). Incrementally growing tissues, such as tusks, otoliths or hair segments, sequentially record dietary Sr, allowing high-resolution reconstruction of mobility histories of the sampled individuals (e.g., Brennan et al., 2015a; Vautour et al., 2015). Other tissues, such as bulk (whole) tooth samples or bones, preserve a snapshot of a specific period in the organism's life, or integrate Sr over longer time periods, respectively, and can therefore provide information about dietary signatures at different stages of an individual's life (reviewed in Makarewicz and Sealy, 2015).

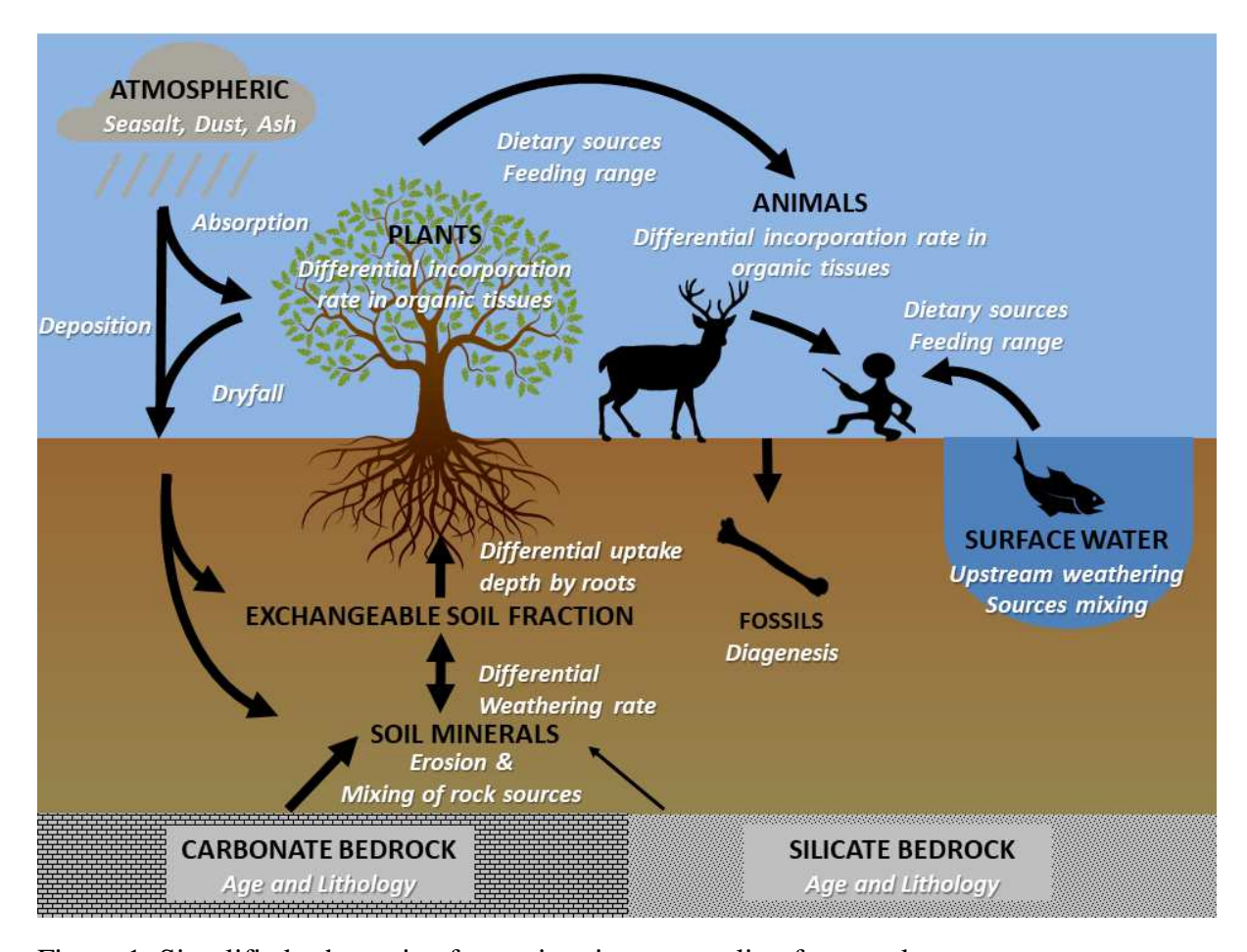


Figure 1: Simplified schematic of strontium isotope cycling from rocks to ecosystems. Capitalized black words correspond to Sr reservoirs and italicized white words correspond to process modifying ⁸⁷Sr/⁸⁶Sr.

3. Strontium isoscapes

3.1 Empirical isoscapes

The most commonly used strategy to create biologically available (bioavailable) ⁸⁷Sr/⁸⁶Sr baselines is to analyze ⁸⁷Sr/⁸⁶Sr in a series of biological samples representing bioavailable Sr pools in a study area (Lengfelder et al., 2019). However, as outlined above, different substrates (e.g., soils, plants, animals, or waters) can integrate ⁸⁷Sr/⁸⁶Sr at different spatiotemporal scales depending on the local geo-environmental conditions. Thus, identifying appropriate substrates can be challenging. We review the pros and cons of each substrate type below.

Modern plants and exchangeable Sr from top soils are the most commonly used substrate to represent local bioavailable Sr because they are easily collected. However, they may sample isotopically discrete pools depending on plant rooting depths (Poszwa et al., 2004). It is also increasingly recognized that application of agricultural fertilizers and limes impacts the natural bioavailable Sr pool (Frei et al., 2020; Maurer et al., 2012; Thomsen and Andreasen, 2019). The extent and frequency of agricultural contamination in baseline samples remains unknown but could seriously complicate the development of bioavailable ⁸⁷Sr/⁸⁶Sr baselines in regions with active or historical agriculture.

Animals with relatively small foraging ranges, such as rodents or deer, are also used to represent the local bioavailable Sr pool (e.g., Burton and Price, 2013). Although animals

integrate Sr over variable spatiotemporal scales, adding some uncertainty in the interpretation, they also offer the advantage of integrating local bioavailable Sr from multiple sources. Isoscapes derived from local animals might therefore be more suitable than those derived from plants or soils to represent the bioavailable Sr sampled by large mammals, including humans (Crowley et al., 2017a). Fortunately, in many cases, the ⁸⁷Sr/⁸⁶Sr of local animals are similar to those of plants and soils, indicating that, at local scales, bioavailable ⁸⁷Sr/⁸⁶Sr signatures are relatively invariant (Flockhart et al., 2015).

Water samples taken from small streams, lakes and rivers have also been used to represent bioavailable Sr pools. As otoliths inherit their ⁸⁷Sr/⁸⁶Sr from the river or lake water in which fish live (Brennan et al., 2015a; Faure et al., 1967), water samples are particularly relevant in freshwater ecology applications (e.g., Brennan et al., 2019). In terrestrial applications, however, water can integrate Sr from larger areas than plants or local animals (Frei and Frei, 2011). Although this spatial integration might help solve some of the lime and fertilizer contamination issues found with other substrates (Frei et al., 2020), it can also complicate the comparison with biological samples. Nevertheless, water samples can provide a good baseline for the ⁸⁷Sr/⁸⁶Sr of terrestrial species exploiting aquatic or riparian habitats (Hamilton et al., 2019).

Once collected, bioavailable ⁸⁷Sr/⁸⁶Sr data are usually interpolated using geostatistical algorithms (e.g., kriging; Copeland et al., 2016; Frei and Frei, 2011; Willmes et al., 2018). Geostatistical algorithms are based on the idea that points closer to each other tend to resemble each other (i.e., spatial autocorrelation). These geostatistical models can also integrate covariates (e.g., geological maps) to further constrain ⁸⁷Sr/⁸⁶Sr patterns (Willmes et al., 2018). Maps derived from geostatistical methods, however, can give ambiguous and inaccurate results due to the challenges of incorporating non-normal and skewed distributions of ⁸⁷Sr/⁸⁶Sr data (Bataille et al., 2018). Another method widely used to produce ⁸⁷Sr/⁸⁶Sr maps is to average ⁸⁷Sr/⁸⁶Sr data over regions with similar bedrock geology (e.g., Evans et al., 2010; Voerkelius et al., 2010). However, this leads to overlap and lack of precision in constructed isoscapes, which limits their usefulness for provenance studies. These limitations can be overcome by increasing the sampling density, but this becomes prohibitively expensive at regional to continental scales.

3.2 Mechanistic isoscapes

A second approach to developing ⁸⁷Sr/⁸⁶Sr isoscapes relies on mechanistic models. This approach leverages geochemical knowledge to predict the evolution of ⁸⁷Sr/⁸⁶Sr in rocks using the radiogenic equation:

314
$$\left(\frac{^{87}Sr}{^{86}Sr}\right)_{rock} = \left(\frac{^{87}Sr}{^{86}Sr}\right)_{i} + \left(\frac{^{87}Rb}{^{86}Sr}\right)_{rock} \left(e^{\bullet t} \bullet 1\right),$$
 (1)

where ${}^{87}\text{Sr}/{}^{86}\text{Sr}$ variability in rocks $({}^{87}\text{Sr}/{}^{86}\text{Sr})_{rock}$ is a function of: 1) The initial ${}^{87}\text{Sr}/{}^{86}\text{Sr}$ [(${}^{87}\text{Sr}/{}^{86}\text{Sr})_i$], which depends on the geological history of the parent rock; 2) Bedrock age (t), which controls the fraction of ${}^{87}\text{Rb}$ that decayed into ${}^{87}\text{Sr}$; and 3) The ${}^{87}\text{Rb}/{}^{86}\text{Sr}$ of the rock [${}^{87}\text{Rb}/{}^{86}\text{Sr})_{rock}$], which varies with lithology.

To simplify the equation, it was first assumed that ⁸⁷Sr/⁸⁶Sr variability in rocks is only a function of rock age (Beard and Johnson, 2000). Using geological maps to estimate the age of bedrock units, these authors predicted ⁸⁷Sr/⁸⁶Sr for bedrock across the USA. Later, Bataille and Bowen (2012) revisited this approach by accounting for distinct ⁸⁷Rb/⁸⁶Sr among rock types. They separated rocks into major lithological categories, specifically distinguishing

between carbonates and silicates, and leveraged geochemical databases to calculate the average ⁸⁷Rb/⁸⁶Sr for each group. These authors also predicted ⁸⁷Sr/⁸⁶Sr variability in rivers across the USA using a first-principles model of chemical weathering to propagate ⁸⁷Sr/⁸⁶Sr from rock to water. This modeling approach yielded notable improvement over the approach used by Beard and Johnson (2000), but the accuracy of both the rock and water isoscapes were not sufficient for most provenance applications.

Using a case study in Alaska, Bataille et al. (2014) improved this mechanistic model by incorporating more detailed lithological categories, including a sub-model for siliciclastic sedimentary rocks. They also integrated an empirically-calibrated chemical weathering model. The resulting model performed well against bedrock and water data. However, the averaging approach, uncertainty of geological maps, and difficulty in calibrating certain rock categories remained major obstacles to the development of ⁸⁷Sr/⁸⁶Sr isoscapes sufficiently accurate for provenance applications.

As mentioned previously, a multitude of coupled processes contribute to mix isotopically distinct Sr sources from rocks to ecosystems. Properly calibrating the interactions of those geological, environmental or biological processes to predict ⁸⁷Sr/⁸⁶Sr in the terrestrial biosphere is a substantial challenge. Bataille et al. (2012) attempted to calibrate a mechanistic bioavailable ⁸⁷Sr/⁸⁶Sr model in the circum-Caribbean region. They demonstrated that bedrock ⁸⁷Sr/⁸⁶Sr predictions diverged from bioavailable ⁸⁷Sr/⁸⁶Sr data in this region (Laffoon et al., 2012) and attempted to calibrate a multi-source model that accounted for the contribution of atmospheric sources. While the model performed well on the existing bioavailable data for the Antilles (Laffoon et al., 2012), additional sampling showed that the contribution of atmospheric deposition was not accurately calibrated in the Bahamas (Schulting et al., 2018).

Developing accurate mechanistic bioavailable ⁸⁷Sr/⁸⁶Sr models requires a coupled parameterization of a multitude of complex processes. Integrating Sr isotope cycling in global land surface models might be a productive avenue to advance the mechanistic approach. However, to date, the lack of accurate, detailed global geological maps remains the major hurdle to more accurate mechanistic ⁸⁷Sr/⁸⁶Sr isoscapes.

3.3 Process-based statistical isoscapes

A third, intermediate approach has been proposed to overcome the limitations of both mechanistic and geostatistical modeling. This approach relies on multivariate random forest regression, a tree based machine-learning algorithm, to integrate empirical data and other geo-environmental covariates into the modeling framework. Bataille et al. (2018) first used random forest regression to predict bioavailable ⁸⁷Sr/⁸⁶Sr across Western Europe. This study integrated a compilation of empirical bioavailable ⁸⁷Sr/⁸⁶Sr data, bedrock model products, and geo-environmental covariates to predict bioavailable ⁸⁷Sr/⁸⁶Sr. The resulting model yielded greatly improved accuracy over mechanistic models while also overcoming the issues encountered with traditional geostatistical methods. More recently, Hoogewerff et al., (2019) used random forest regression to predict ⁸⁷Sr/⁸⁶Sr for agricultural top soils across Europe using previously collected geochemical soil data and newly generated ⁸⁷Sr/⁸⁶Sr data from selected soils of the GEMAS project (i.e., Geochemical Mapping of Agricultural and Grazing Land Soil). This method yielded excellent results, predicting bioavailable ⁸⁷Sr/⁸⁶Sr with both high precision and accuracy. However, the model was limited by the availability of high-resolution geochemical soil surveys.

In freshwater environments, Brennan et al. (2016) proposed using spatial stream network models to predict ⁸⁷Sr/⁸⁶Sr in river water. This statistical approach accounts for the unique spatial correlation structure in rivers (e.g., flow direction, branching) while also providing a quantitative framework for assessing the contribution of in-stream processes (e.g., downstream transport) and landscape processes (e.g., climate, geology) on observed ⁸⁷Sr/⁸⁶Sr patterns. The application of this method was a break-through in freshwater ⁸⁷Sr/⁸⁶Sr isoscaping, improving accuracy by an order of magnitude over both mechanistic (Bataille et al., 2014) and geostatistical models (Hegg et al., 2013).

4. Building process-based global bioavailable strontium isoscape

4.1 Global compilation

368

369

370

371

372

373

374375

376

377

378

379

380

381

382

383

384

385

386

387

388

389

390

391

392

393

394395

396

397

398

4.1.1 Compilation description

To date, no researchers have attempted global bioavailable ⁸⁷Sr/⁸⁶Sr modeling. Here we leverage a new global data compilation, mechanistic models, and auxiliary variables integrated in a multivariate random forest regression framework to predict bioavailable ⁸⁷Sr/⁸⁶Sr at the global scale. The dataset used in our study is a compilation of 17,240 published and unpublished ⁸⁷Sr/⁸⁶Sr analyses from 278 individual studies spanning 8,476 individual locations across the globe (Fig. 2). Unpublished data include 279 bioavailable ⁸⁷Sr/⁸⁶Sr from Madagascar (see supplementary material Appendix B) and 70 surface waters from Cook Inlet Alaska (see supplementary material Appendix C). The compiled database is available in supplementary material Table S1 (along with the full citations of the original sources from which the data sets were derived), and is being integrated in the IsoBank repository (Pauli et al., 2017). The data can be filtered by country, sample type (several levels), or analytical substrate. Local data come from 3,249 plants, 2,598 soils, 2,335 local animals (bone, dentine, enamel, snail shell), and 4,813 surface waters. The remaining samples include migratory or highly mobile animals, humans, and dust that could be useful in other applications. The database includes latitude and longitude data for each individual sample. In the majority of cases, geographic coordinates were reported by the authors in the publication. When these were not included, we used Google Earth to georeference reported geographic information (e.g., maps or locality names). When necessary, authors of publications were contacted to clarify locality information. The method of georeferencing and its associated uncertainty are reported in the database (Table S1).

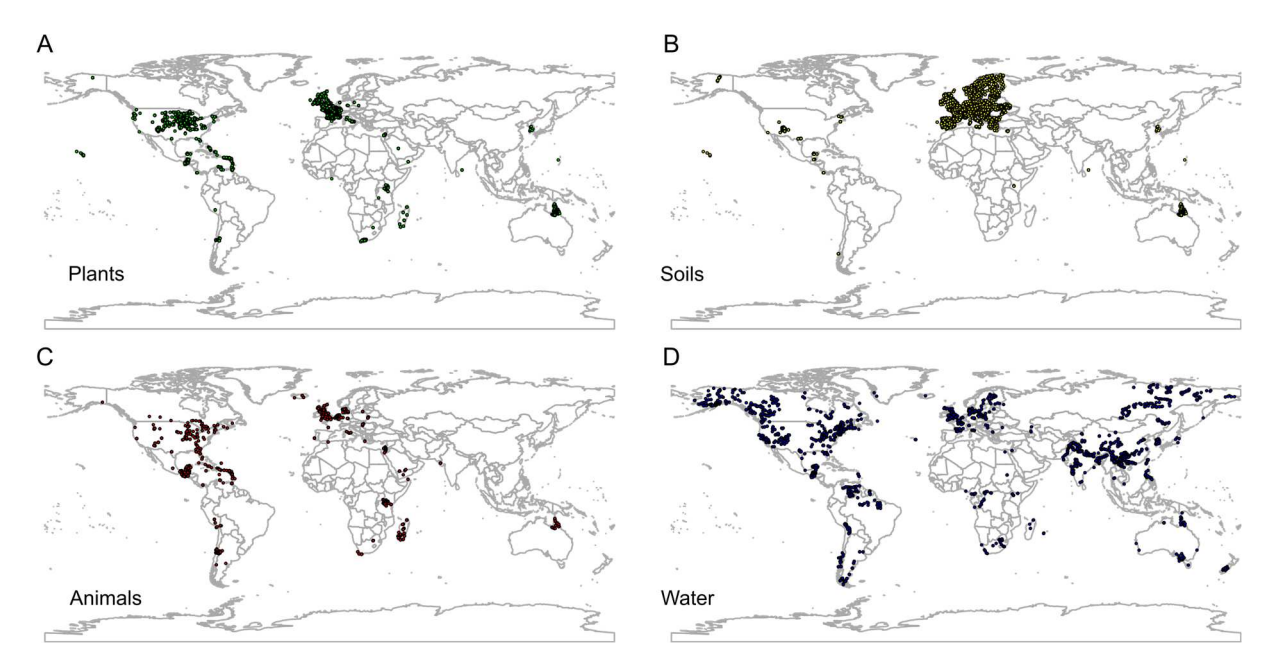


Figure 2: Global compilation of ⁸⁷Sr/⁸⁶Sr data by substrate. A) Plants, B) Soils, C) Animals and D) Water.

4.1.2 Geographic biases and sample distribution

The sampling density, and geographic distribution of bioavailable ⁸⁷Sr/⁸⁶Sr data vary tremendously across the globe. Most samples are from regions with a high archeological interest (e.g., Mesoamerica) or strong research funding programs (e.g., Europe, USA). Plant and local animal samples are concentrated in Europe, the USA and the circum-Caribbean region. Soil samples are highly concentrated in Europe with close to half coming from the published GEMAS dataset (Hoogewerff et al., 2019). Water samples are more broadly distributed and include most large rivers of the world; this reflects the 50 years of hydrological research using ⁸⁷Sr/⁸⁶Sr geochemistry. The sampling strategy also varied among studies. In some, samples from different substrates were collected opportunistically depending on research funds and accessibility (e.g., Laffoon et al., 2012), while in others, samples from one substrate were collected systematically on a regular grid (e.g., Hoogewerff et al., 2019). Additionally, even though the global compilation is extensive and covers areas representing different climatic zones, many regions remain strongly under-sampled due to restricted access, extreme climate conditions, or political reasons. These geographic biases will propagate in models calibrated using this global compilation (e.g., regions with low sample density will be poorly calibrated relative to regions with high sample density).

4.1.3 Descriptive statistics

Plants, soils and local animals display similar distributions of 87 Sr/ 86 Sr, with Quartile 1 = 0.7084 ± 0.0001, median = 0.7095 ± 0.0003, and Quartile 3 = 0.711 ± 0.0004 (Fig. 3). More than 90% of the samples have 87 Sr/ 86 Sr that falls within a tight range of 0.706 ± 0.001 to 0.720 ± 0.001 (Fig. 3). Variability in water is slightly larger with Quartile 1 = 0.7089, median = 0.7110, Quartile 3 = 0.7155, and a 90% interval range from 0.706 to 0.7396. This difference in range between water and other substrates is likely due to spatial sampling biases (Fig. 2). Many of the water samples compiled in the database are from older radiogenic geological regions including the Himalayas, Canadian craton, Scandinavian cratons and Russian cratons (Fig. 2). This geographic distribution contrasts with that of plants, soils and

local animals that were mostly sampled from flatter areas, agricultural regions and younger geological regions.

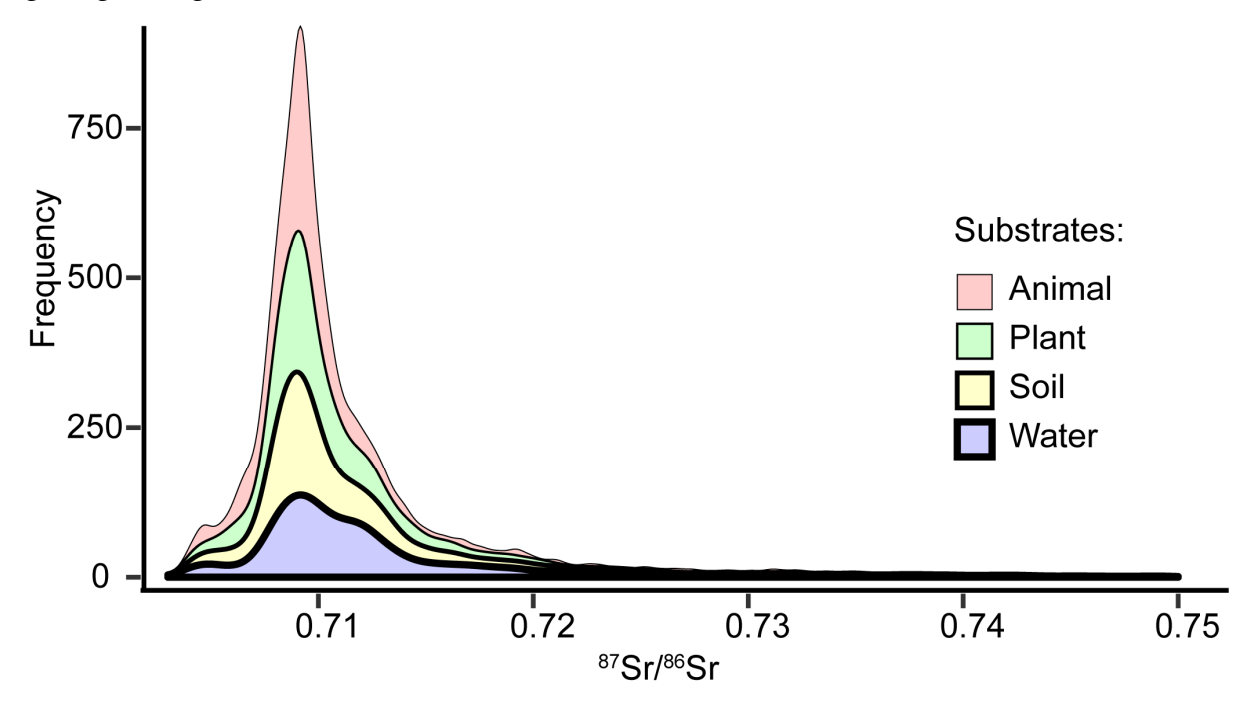


Figure 3: Distribution of ⁸⁷Sr/⁸⁶Sr variability by substrate (stacked). The x-axis is cut at 0.750 to facilitate visualization but more some water samples fall beyond that range.

4.1.4 Intra-site variability

We explored intra-site variability in bioavailable ⁸⁷Sr/⁸⁶Sr by calculating the standard deviation of ⁸⁷Sr/⁸⁶Sr among samples at each location where more than one sample/substrate was collected. This intra-site variability is an important measure as it represents the maximum accuracy a model could reach. As noted in previous studies (Bataille et al., 2018; Hoogewerff et al., 2019), there is a clear trend of increasing variance with increasing ⁸⁷Sr/⁸⁶Sr for plants, soils and animals (Fig. 4). Bioavailable ⁸⁷Sr/⁸⁶Sr is most variable for sites dominated by very old felsic rock units (e.g., cratons) with ratios >0.710. The minimum variance is found between 0.707 and 0.709, corresponding to ⁸⁷Sr/⁸⁶Sr of carbonate units (Fig. 4). Sites with ⁸⁷Sr/⁸⁶Sr <0.707 (typical of younger and/or mafic geologies) have slightly higher variance than sites dominated by carbonates. Combining plants, soils and local animals, the Root Mean Squared Error (RMSE) of intra-site variability is 0.001. However, this RMSE is lower than 0.0005 when using only bioavailable ⁸⁷Sr/⁸⁶Sr < 0.710.

The positive correlation between predicted bioavailable ⁸⁷Sr/⁸⁶Sr and RMSE is consistent with the lognormal distribution of ⁸⁷Sr/⁸⁶Sr in the geosphere. As the age of a rock unit increases, the different minerals composing this unit have increasingly divergent ⁸⁷Sr/⁸⁶Sr. Differential weathering of those minerals can considerably increase variability in ⁸⁷Sr/⁸⁶Sr for soils at radiogenic sites even at the very local scale (Clow et al., 1997). In addition, felsic rocks tend to weather slowly, which means there may be a higher relative contribution of bioavailable Sr from exogenous sources (e.g., dust) (Hoogewerff et al., 2019).

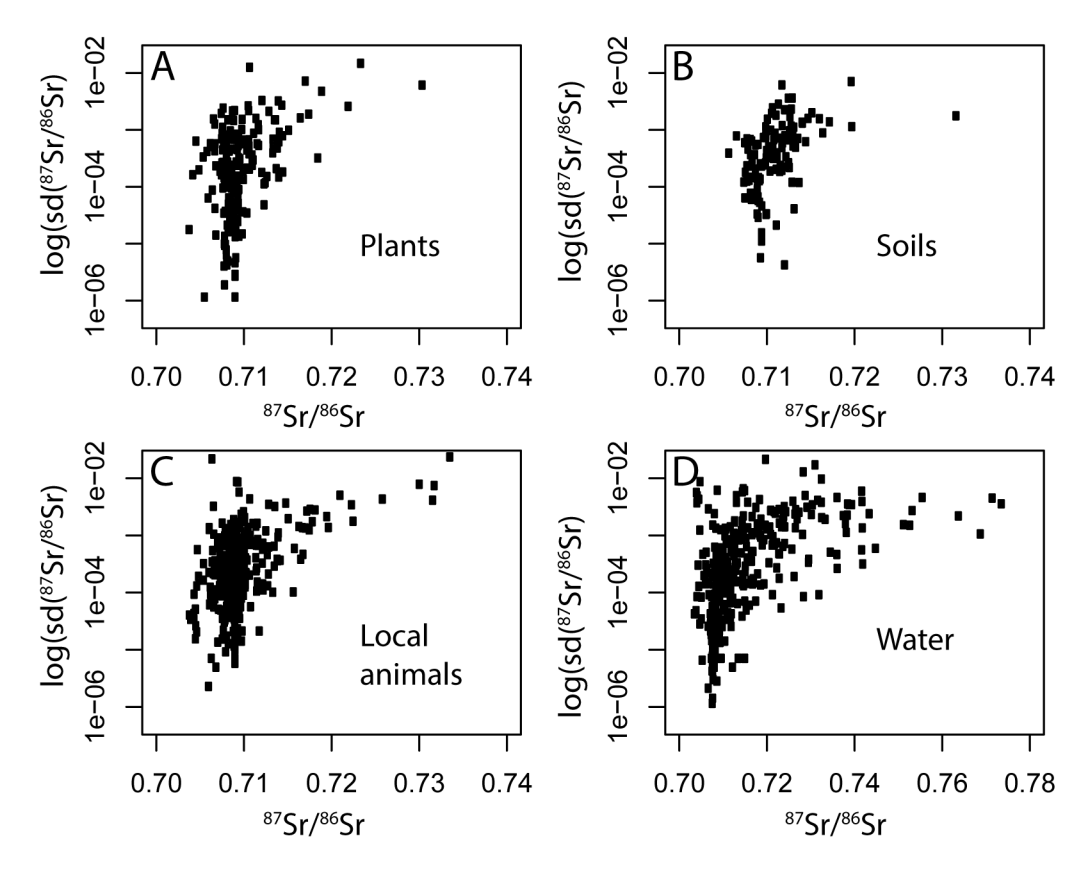


Figure 4. Within-site ⁸⁷Sr/⁸⁶Sr variability by substrate. A) Plants, B) Soils, C) Local animals and D) Water.

4.2 Mechanistic bedrock model

454

455

456

457

458

459

460

461

462

463

464

465

466

467

468

469 470

471

472

473

474 475

476

477

478

We applied the published model formulation of Bataille et al. (2014) at a global scale using the GLiM geological map as the primary source for geological information. (Fig. 5). This bedrock model predicts the median, Quartile 1 and Quartile 3 of 87Sr/86Sr for bedrock at present-day. As the GLiM geodatabase does not contain numerical age information (Hartmann and Moosdorf, 2012), we converted age descriptor to a range of numerical values using the geological timescale (Walker et al., 2013; see supplementary material Table S2). For more information on the exact parameterization steps of the bedrock model, refer to the supplementary material in Bataille et al. (2014), including Tables A1 and A3. Predicted bedrock ⁸⁷Sr/⁸⁶Sr follows the expected trends, with higher ⁸⁷Sr/⁸⁶Sr in older cratonic settings and lower ⁸⁷Sr/⁸⁶Sr in arc settings (Fig. 5). However, the bedrock model predictions also reflect the limitations of the GLiM geodatabase. The GLiM was constructed by compiling geological maps at different resolutions with an "average" resolution of 1:3 750 000. It divides lithologies into 16 major classes, separating mafic, intermediate and felsic plutonic and volcanic rocks, metamorphic rocks, carbonates, evaporites, silicates, and mixed carbonate/silicate sediments. Of particular relevance for predicting ⁸⁷Sr/⁸⁶Sr in rocks, secondary lithological descriptors also report the presence of carbonates, evaporites and loess. However, reporting of secondary lithologies is inconsistent among countries (and frequently absent). Similarly, the definition of bedrock can differ between countries, with some surveys mapping surficial sediments (e.g., glacial till) as bedrock whereas other reserve bedrock mapping to the solid rock unit underlying unconsolidated sediments. Consequently, irregularities in predicted ⁸⁷Sr/⁸⁶Sr, reflecting different mapping methods, resolution and

accuracy are often observed at political borders (e.g., Canada, USA). These inaccuracies cannot be resolved until high resolution harmonized geological maps are produced at the global scale. Another major source of uncertainty in this bedrock model is that the bedrock ages (Table S2) mean different things for different lithologies (e.g., crystallization age for intrusive rocks, eruptive ages for volcanic rocks, last higher-grade metamorphic overprint of metamorphic rocks, and depositional age for sedimentary rocks). Consequently, some lithologies (i.e., metamorphic, sedimentary), might contain significantly older minerals than the overall age of the geologic unit (e.g., a recently deposited sediment might have zircon grains that are billion years old). This can lead to large uncertainties in predicted bedrock ⁸⁷Sr/⁸⁶Sr.

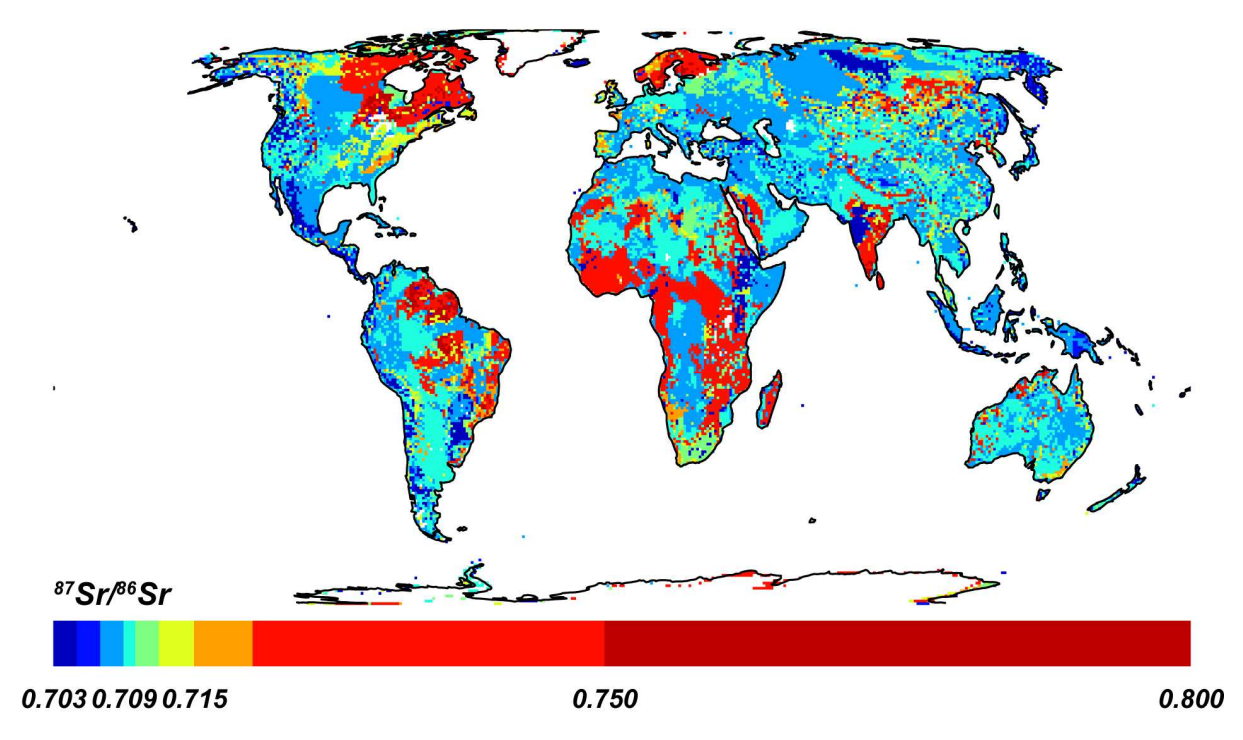


Figure 5: Global map of predicted ⁸⁷Sr/⁸⁶Sr in bedrock following the formulation of Bataille et al. (2014)

4.3 Other auxiliary data.

We assembled data on selected covariates that represent the main factors that impact variability in bioavailable ⁸⁷Sr/⁸⁶Sr: Bedrock ages (see section 4.2), terrane age, surficial geology type, soil properties, aerosol deposition, relief, climate, and agricultural activity (Table 1). This series of covariates expands on Bataille et al. (2018) by including global nitrogen and phosphorus fertilization (Potter et al., 2010), surficial deposits (Börker et al., 2018), global mean annual temperature (Hijmans et al., 2005), and an updated raster of global sea salt aerosol deposition (Vet et al., 2014).

Table 1: List of geological, climatic, environmental and anthropogenic variables used in the multivariate regression. D = Discrete; C = Continuous; GLiM = Global Lithological Map; CCSM.3 = Community Climate System Model 3; SRTM = Shuttle Radar Topography Mission

Variables	Description	Resolution	Type	Source
r.maxage_geol	GLiM age attribute	1 km	D	(Hartmann and Moosdorf,

	(Myrs)			2012)
r.minage_geol	GLiM age attribute (Myrs)	1 km	D	(Hartmann and Moosdorf, 2012)
r.meanage_geol	GLiM age attribute (Myrs)	1 km	D	(Hartmann and Moosdorf, 2012)
r.age	Terrane age attribute (Myrs)	1 km	D	(Mooney et al., 1998)
r.GUM	Global unconsolidated sediment map	1 km	С	(Börker et al., 2018)
r.ssaw	Multi-models average sea salt wet deposition (kg.ha ⁻¹ .yr ⁻¹)	1°×1°	С	(Vet et al., 2014)
r.ssa	Multi-models average Sea salt wet+dry deposition (kg.ha ⁻¹ .yr ⁻¹)	1°×1°	С	(Vet et al., 2014)
r.dust	Multi-models average (g.m ⁻² .yr ⁻¹)	1°×1°	С	(Mahowald et al., 2006)
r.elevation	SRTM (m)	90 m	C	(Jarvis et al., 2008)
r.cec	Cation Exchange Capacity	250 m	С	(Hengl et al., 2017)
r.ph	Soil pH in H ₂ O solution (x10)	250 m	С	(Hengl et al., 2017)
r.phkcl	Soil pH in KCl solution (x10)	250 m	С	(Hengl et al., 2017)
r.clay	Clay (weight %)	250 m	С	(Hengl et al., 2017)
r.orc	Soil organic carbon (weight %)	250 m	С	(Hengl et al., 2017)
r.bulk	Bulk density (kg m ⁻³)	250 m	С	(Hengl et al., 2017)
r.bouguer	WGM2012_Bouguer	2 min	С	(Balmino et al., 2012)
r.map	Mean annual precipitation (mm.yr-1)	30-arc sec	С	(Hijmans et al., 2005)
r.mat	Mean annual temperature (°C)	30-arc sec	С	(Hijmans et al., 2005)
r.nfert	Global Nitrogen Fertilization	30-arc sec	С	(Potter et al., 2010)
r.pfert	Global Phosphorus Fertilization	30-arc sec	С	(Potter et al., 2010)

- 4.4 Random forest regression and spatial predictions
- 4.4.1 Random forest regression procedure

All statistical analyses and figures from this manuscript are conducted in R programming language version Rx64 3.4.2. (https://www.r-project.org/). An example of R-script is available in supplementary material Script S1. We used random forest regression to predict bioavailable ⁸⁷Sr/⁸⁶Sr variability using the compiled database (Table S1), the bedrock model and the covariates described above following the framework developed by Bataille et al. (2018) and the caret package (Kuhn, 2008). Random forest is a tree-based machine-learning algorithm trained by bootstrap sampling and random feature selection. In a decision tree, a random subset of the dataset is entered, and then each predictor splits the original dataset into smaller and smaller sets at nodes in the tree. Random forest takes this idea to the next level by constructing an ensemble of trees (or forest) using bootstrapping. Specifically, random

forest creates multiple decision trees on different data samples where sampling is done with replacement to prevent overfitting. To make fair use of all potential predictors, the number of features split at each node of a tree is limited to some user-defined threshold. Ultimately, random forest aggregates the results of these decision trees to predict the mean value of the response variable, in our case the bioavailable ⁸⁷Sr/⁸⁶Sr. Random forest is a practical algorithm that requires very little pre-processing. No transformation is required for ⁸⁷Sr/⁸⁶Sr data as random forest makes no assumptions about the data distribution and residual heteroscedasticity. Random forest can also directly integrate categorical variables in multivariate regression so long as they do not have too many classes (Strobl et al., 2007).

In our approach, random forest regression models were optimized using root mean squared error (RMSE) as the primary metric and a 10-fold repeated cross-validation scheme with 5 repetitions using 80% of the data for training at each iteration. Variable selection was performed using the *VSURF* package (Genuer et al., 2015). Once a model is optimized, we used variable importance purity measure and partial dependence plots to describe the relationships between the selected predictors and predicted ⁸⁷Sr/⁸⁶Sr. Ultimately, the ⁸⁷Sr/⁸⁶Sr isoscapes were generated using the best performing random forest regression model for each substrate (plant, soil, local animal, water) and the associated predictors.

Spatial uncertainty assessment is critical for using isoscapes in continuous-probability surface models of geographic assignment (Wunder, 2012). However, while random forest provides a mean ⁸⁷Sr/⁸⁶Sr prediction using the selected predictors, there are no built-in features to assess spatially explicit model uncertainty. To circumvent this issue, we calculated an uncertainty function for each trained model that relates the mean absolute residual values to predicted ⁸⁷Sr/⁸⁶Sr (e.g., Fig. 7D). This function reflects the observation that uncertainty tends to increase with increasing predicted ⁸⁷Sr/⁸⁶Sr. While using quartile random forest regression to calculate the interquartile range would be ideal (as in Bataille et al. 2018), this method is computationally intensive. Our uncertainty function provides an average standard deviation at each pixel that that can be directly used in probabilistic provenance assignments (Wunder, 2012).

4.4.1 Comparison of random forest regressions among substrates

We applied random forest regression independently to the plant, soil, local animal, and water datasets (Fig. 6). All substrates show very similar predictors after the *VSURF* variable selection step (Fig. 7 and Appendix A). Random forest models applied to plant, soil, and local animals perform similarly, whereas the model using only water data has a lower performance (Fig. 6). In our approach, we extracted the values of covariates using site location and the closest underlying 1 km² pixel. This approach is appropriate for plants, soils and local animals because these substrates integrate Sr sources over local spatial scales. However, river water frequently integrates Sr sources over much larger spatial scales and from groundwater sources that are not represented in geological maps. Although extracting local environmental conditions at 1 km² pixel resolution might be appropriate for small streams, it becomes inaccurate for large rivers, which comprise a large proportion of the database. Future predictive work focused on surface waters could use watershed-integrated covariates to address this issue. Another reason for the lower model performance for water samples, and to a lesser degree soil samples, is their broader distribution of ⁸⁷Sr/⁸⁶Sr (due to samples coming from a larger variety of geologies; Fig. 6B and 6D).

To simplify visualization, we trained the main model using a dataset combining plant, soil and local animal ⁸⁷Sr/⁸⁶Sr (herein called the "combined local bioavailable ⁸⁷Sr/⁸⁶Sr dataset"). We excluded the water samples from this subset due to the difference in spatial integration represented by this substrate. Model predictors, results, and residuals for individual substrates including plant, soil, local animal, and water are available in supplementary material Appendix A.

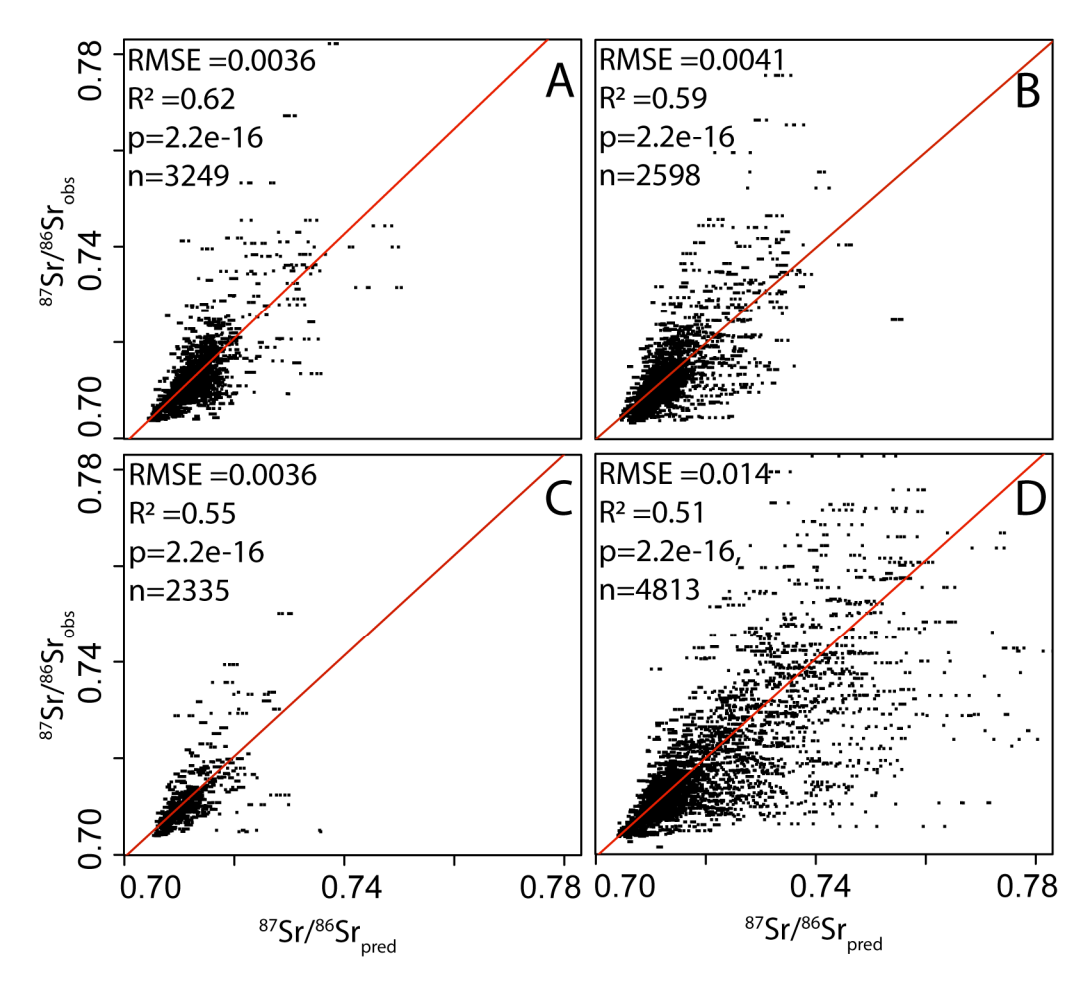


Figure 6: n-fold cross-validation for random forest model by substrate. A) Plants, B) Soils, C) Local animals, and D) Water. RMSE = Root Mean Square Error. Red lines are best fit linear models.

4.4.2 Global bioavailable model performance

After *VSURF* feature selection, Bataille et al. (2014)'s model products (r.srsrq1 and r.srsrq3) and geological variables (r.age, r.minage_geol) from the GLiM database were the dominant predictors of the combined local bioavailable ⁸⁷Sr/⁸⁶Sr dataset (Fig. 7A). Other important predictors of ⁸⁷Sr/⁸⁶Sr included dust and sea salt aerosol deposition (r.dust and r.ssaw), elevation (r.elevation), climate variables (r.pet and r.mat) and soil properties (r.ph and r.clay) (Fig. 7A). After n-fold cross validation, the bioavailable ⁸⁷Sr/⁸⁶Sr model explains 60% of the variance, with a RMSE of 0.0034 over the dataset (Fig 7B). The value of 0.0034 represents < 10% of the full range of observed bioavailable ⁸⁷Sr/⁸⁶Sr over the compiled dataset. However, this uncertainty is not uniform across the prediction range. For low bioavailable ⁸⁷Sr/⁸⁶Sr (<0.710), the RMSE is low (<0.001), with lowest uncertainty values for

⁸⁷Sr/⁸⁶Sr ~0.709 (Fig. 7C and 7D). However, as ⁸⁷Sr/⁸⁶Sr increases, the absolute values of residuals increase (Fig. 7C and 7D). This observation conforms with previous studies (e.g., Bataille et al. 2018) that ecosystems developing on older, more felsic rock units (e.g., cratons, Precambrian metasediments) not only have higher intra-site ⁸⁷Sr/⁸⁶Sr variability (Fig. 4) but are also much harder to predict accurately. Ecosystems developing on carbonate units have the lowest intra-site ⁸⁷Sr/⁸⁶Sr variability (Fig. 7D).

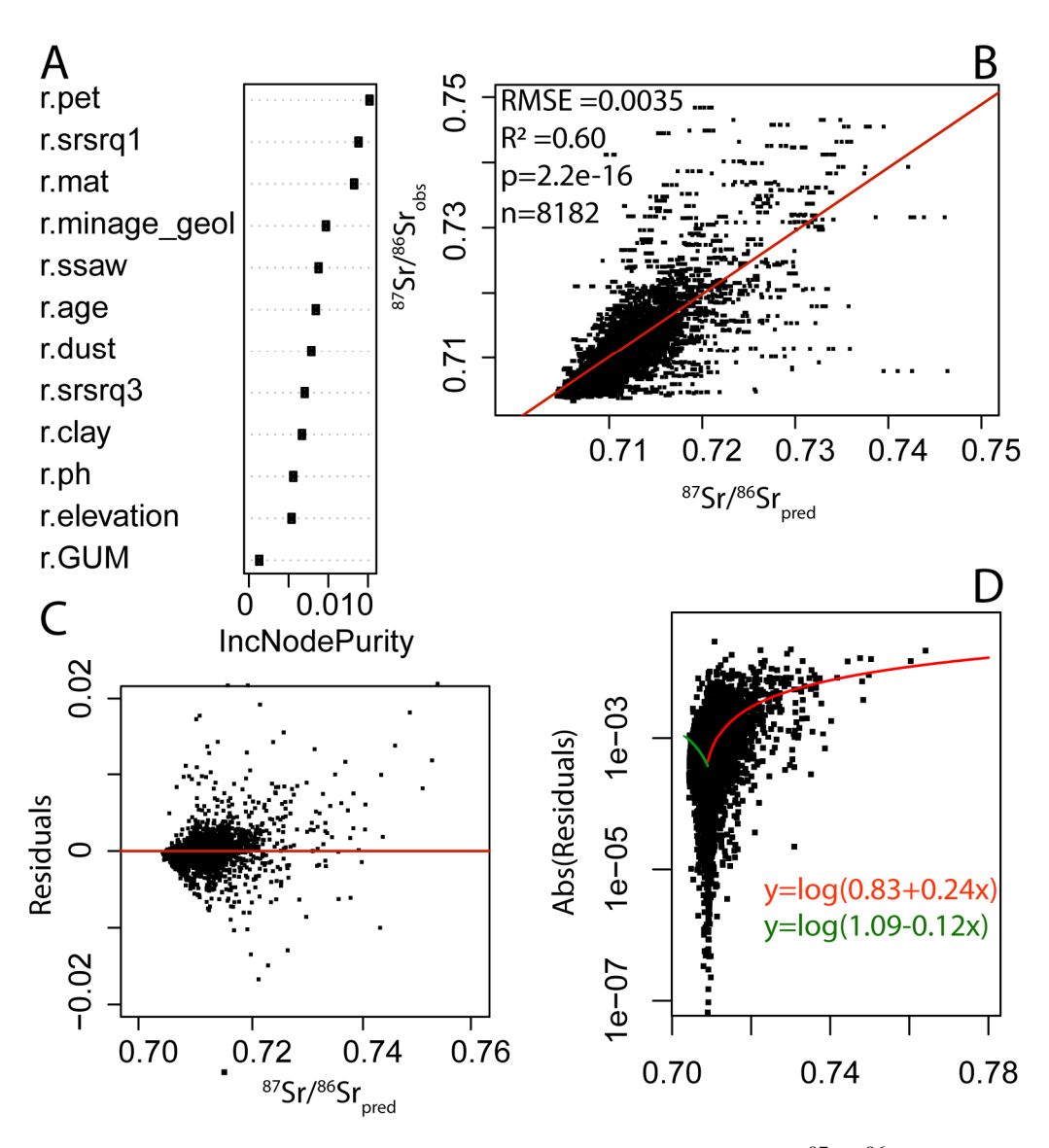


Figure 7: Random forest regression model for the bioavailable ⁸⁷Sr/⁸⁶Sr dataset combining plant, soil and local animal samples: A) Variable importance plot after selection of predictors by *VSURF*; B) N-fold cross-validation results with best fit linear model (red line); C) Residuals against ⁸⁷Sr/⁸⁶Sr_{pred}; D) Absolute residual values (logscale) against ⁸⁷Sr/⁸⁶Sr_{pred}. Green line indicates the best fit non-linear model between 0.703 and 0.709; red line indicates the best fit non-linear model between 0.780. Refer to Table 1 for predictor names.

4.4.3 Predictors of bioavailable ⁸⁷Sr/⁸⁶Sr variability

We used a partial dependence plot to investigate the relationship between bioavailable ⁸⁷Sr/⁸⁶Sr and the selected predictors for the combined local bioavailable ⁸⁷Sr/⁸⁶Sr dataset (Fig. 8). As expected bioavailable ⁸⁷Sr/⁸⁶Sr increased with increasing bedrock ⁸⁷Sr/⁸⁶Sr (r.srsrq1 and r.srsrq3), as well as the age of geological units (r.minage_geol) and terranes (r.age). These relationships confirm the dominance of age and lithology of rock units in controlling bioavailable ⁸⁷Sr/⁸⁶Sr at the global scale (Bataille et al., 2014; Bataille and Bowen, 2012). However, we also observe a lack of association between geological variables and bioavailable ⁸⁷Sr/⁸⁶Sr for older rock units (Fig. 8). This observation confirms that the current set of geological predictors (i.e., bedrock model products and GLiM products) are inadequate for explaining the large variability of bioavailable ⁸⁷Sr/⁸⁶Sr for rock units with higher ⁸⁷Sr/⁸⁶Sr.

A few additional geological predictors influence bioavailable ⁸⁷Sr/⁸⁶Sr in the combined local bioavailable ⁸⁷Sr/⁸⁶Sr dataset, including surficial deposit types (r.GUM), elevation (r.elevation), and soil proprieties (r.ph and r.clay). For surficial deposits, higher bioavailable ⁸⁷Sr/⁸⁶Sr is found in regions dominated by siliciclastic surficial sedimentary units, including unconsolidated alluvial, fluvial, glacial and aeolian sediments (Fig. 8), whereas lower ⁸⁷Sr/⁸⁶Sr is observed for marine sediments (evaporites and carbonates), and pyroclastic units (Fig. 8). While the global unconsolidated sediment map (GUM) is a significant predictor of bioavailable ⁸⁷Sr/⁸⁶Sr, its predictive potential could be improved in future modeling efforts by characterizing the parent rock of each sedimentary unit using detrital zircon databases. Bioavailable ⁸⁷Sr/⁸⁶Sr data also show a positive relationship with elevation, probably due to the preferential uplift and exposure of older radiogenic units during orogenies. Bioavailable ⁸⁷Sr/⁸⁶Sr decreases with soil pH and soil clay content, likely underlining the dominance of carbonate weathering in more basic soils. We did not find any significant relationship between N and P fertilization inputs and bioavailable ⁸⁷Sr/⁸⁶Sr. However, this does not rule out the potential impact of liming on bioavailable ⁸⁷Sr/⁸⁶Sr in some settings (Thomsen and Andreasen, 2019).

Multiple climate variables also strongly influence bioavailable ⁸⁷Sr/⁸⁶Sr. Bioavailable ⁸⁷Sr/⁸⁶Sr shows an exponential increase with both mean annual temperature (r.mat) and potential evapotranspiration (r.pet). These relationships are likely coincidental and reflect the strong sampling bias towards hot regions located on Precambrian cratons (e.g., Madagascar, South Africa, and Tanzania; Fig. 2). The relationship between dust deposition (r.dust) and bioavailable ⁸⁷Sr/⁸⁶Sr is complex. Bioavailable ⁸⁷Sr/⁸⁶Sr decreases for moderate dust deposition but increases at higher deposition rates. This relationship is probably associated with the different isotopic signatures of dust sources: Dust with elevated ⁸⁷Sr/⁸⁶Sr dominates in regions with the highest deposition rate (e.g., Sahara Desert) while lower ⁸⁷Sr/⁸⁶Sr and deposition rates are observed in other arid regions (e.g., Southwestern USA, South America). Last, bioavailable ⁸⁷Sr/⁸⁶Sr converges towards 0.71 with increasing sea salt aerosol deposition, which is consistent with inputs of marine-derived Sr in coastal ecosystems.

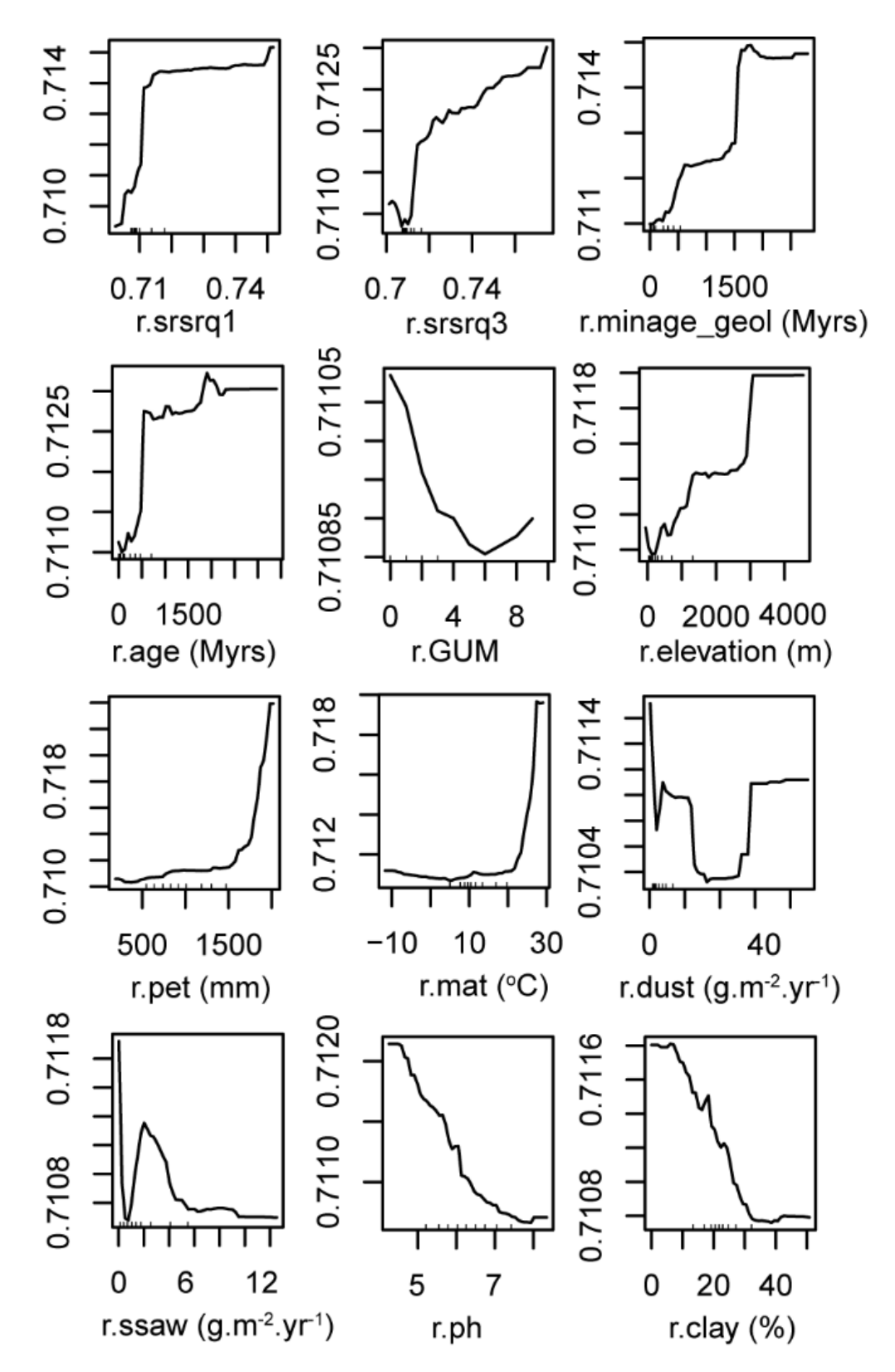


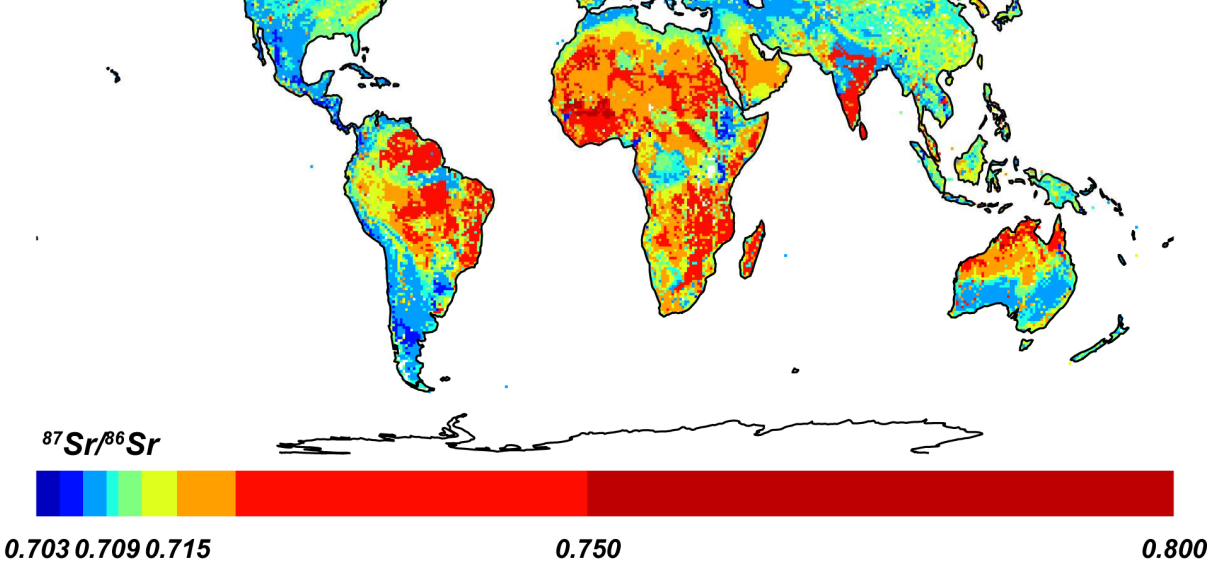
Figure 8: Partial dependence plots between predictors (x-axis) and predicted bioavailable 87 Sr/ 86 Sr (y-axis) from random forest regressions using the combined local bioavailable 87 Sr/ 86 Sr dataset. Refer to Tables 1 for description and sources of each covariate. Hash marks along the x axis show covariate sample decile values. For r.GUM, the x-axis represents unconsolidated sediment categories with 0 = No surficial sediment reported; 1 = Colluvial; 2 = Colluvial

```
    Eolian; 3 = Glacial; 4 = Lacustrine; 5 = Marine; 6 = Organic; 7 = Evaporite; 8 =
    Pyroclastics; 9 = Coastal.
```

4.4.4 Patterns in bioavailable ⁸⁷Sr/⁸⁶Sr variability

We used the random forest regression results from the combined local bioavailable ⁸⁷Sr/⁸⁶Sr dataset to predict bioavailable ⁸⁷Sr/⁸⁶Sr at the global scale (Fig. 9). The spatial uncertainty map associated with these predictions is calculated using the relationship between absolute residual value and bioavailable ⁸⁷Sr/⁸⁶Sr predictions (Fig. 7D). The median bioavailable ⁸⁷Sr/⁸⁶Sr predictions show similar spatial patterns to predictions by the mechanistic global bedrock model (Fig. 5). High bioavailable ⁸⁷Sr/⁸⁶Sr is predicted for cratonic and mountainous regions dominated by older, felsic bedrock units, as well as arid regions across the Sahara Desert and the Middle East, where dust with elevated ⁸⁷Sr/⁸⁶Sr substantially contributes to the bioavailable Sr pool. Low ⁸⁷Sr/⁸⁶Sr is found in arc settings and carbonate-dominated regions. However, the overall variability in predicted bioavailable ⁸⁷Sr/⁸⁶Sr is lower than the bedrock model. This buffering is consistent with our knowledge of Sr isotope cycling from rocks to ecosystems. The majority of predicted bioavailable ⁸⁷Sr/⁸⁶Sr falls within a tight range from 0.7085 to 0.711, and converges towards 0.710 (Fig. 3).

This convergence towards 0.710 likely reflects the mixing of Sr from two main sources: 1) Siliciclastic Sr and 2) marine Sr. Siliciclastic sediments are volumetrically the dominant parent material to most ecosystems (Hartmann and Moosdorf, 2012). As described earlier, silicates have a broad range of ⁸⁷Sr/⁸⁶Sr ranging from 0.703 in mafic environments to more than 0.720 in older felsic units with an average upper crust value of 0.716. However, while silicates constitute the main parent material to most soils, they contain little Sr, weather slowly, and do not represent the dominant source of Sr to most ecosystems. Conversely, carbonates and evaporites cover only a small portion of the Earth surface (Hartmann and Moosdorf, 2012), but they contain more Sr and weather faster than other rock types (Palmer and Edmond, 1992). Consequently, marine Sr, with its comparatively tight isotopic range (0.707-0.709) tends to contribute to most ecosystems across the globe through direct weathering of carbonate units, weathering of trace carbonates in shales, deposition of carbonate dust, and/or addition of sea salt aerosols.



670 Figure 9: Global map of predicted bioavailable ⁸⁷Sr/⁸⁶Sr from random forest regression.

- 5. Testing the global bioavailable ⁸⁷Sr/⁸⁶Sr isoscape
- 5.1 Regional dataset

671

672

673

674

675

676

677

678

679

680

681

682

683

684

685

686

687

688

689

690

691

692

693

694

695 696

697

We tested the performance of the model in two regions with different geological settings and sampling density to provide guidance on how to use this global bioavailable ⁸⁷Sr/⁸⁶Sr isoscape. First, we used data collected through the GEMAS project (Hoogewerff et al., 2019) to test the performance of the global model in a data-rich region. To date, GEMAS is the most systematic and comprehensive continental-scale dataset of bioavailable ⁸⁷Sr/⁸⁶Sr. The dataset includes close to 1,200 soil samples from a large collection of grazing (Gr) and agricultural (Ap) soils in Europe. It also covers a broad geographic range, including Eastern and Northern Europe with diverse geology, climate and environmental conditions (e.g., Baltic Shield), making the dataset ideal for testing the performance of the global model in a datarich region. Second, we examined bioavailable ⁸⁷Sr/⁸⁶Sr for the island of Madagascar. The dataset includes published data (Burney et al., 2020; Crowley et al., 2018, 2017b; Crowley and Godfrey, 2019) as well as previously unpublished data from plants, modern rodents and subfossil local animals (n = 279) at 54 individual locations (See supplementary material Appendix B). Madagascar, and Africa as a whole, is a data-poor region for bioavailable ⁸⁷Sr/⁸⁶Sr. The closest bioavailable ⁸⁷Sr/⁸⁶Sr dataset in our global database is from South Africa (Copeland et al., 2016). Additionally, Madagascar is geologically heterogeneous and complex. Its bedrock geology spans Earth's history, from the Archean to the Quaternary (reviewed in Crowley and Sparks, 2019). Most of the island is dominated by Precambrian units with varied lithologies. Variable climate and rugged topography further complicate Sr isotope cycling from rocks to ecosystems. Ultimately, Madagascar is one of the regions of the world where bioavailable ⁸⁷Sr/⁸⁶Sr is likely to be highly heterogeneous, which will likely affect the predictive accuracy of our global model.

5.2 Model comparison approach

We compared the performance of four modeling approaches to predict bioavailable ⁸⁷Sr/⁸⁶Sr for the GEMAS dataset and the newly amassed Madagascar dataset. First, we compared each bioavailable dataset to bedrock model predictions. Second, we compared the bioavailable ⁸⁷Sr/⁸⁶Sr datasets to predictions from our non-locally calibrated global random forest regressions. For these models, we applied random forest regression using the global bioavailable ⁸⁷Sr/⁸⁶Sr compilation (i.e., combined local bioavailable ⁸⁷Sr/⁸⁶Sr dataset) but selectively removed bioavailable data from GEMAS or from Madagascar depending on the location tested. The goal of this step was to assess the possibility of extrapolating global model predictions for an area with little or no bioavailable ⁸⁷Sr/⁸⁶Sr data. Third, we compared the bioavailable ⁸⁷Sr/⁸⁶Sr datasets to the global bioavailable ⁸⁷Sr/⁸⁶Sr model calibrated using the global compilation including ⁸⁷Sr/⁸⁶Sr data from GEMAS and Madagascar. Lastly, we compared the bioavailable ⁸⁷Sr/⁸⁶Sr datasets to locally calibrated models. For these models, we applied random forest regression using only the GEMAS or newly amassed Madagascar ⁸⁷Sr/⁸⁶Sr dataset, respectively (Fig. 9).

5.3 Results of model comparisons

5.3.1 Europe

In Europe, we found that the bedrock model alone explains 30% of the variance in the GEMAS ⁸⁷Sr/⁸⁶Sr dataset (Fig. 10A), confirming that bedrock ⁸⁷Sr/⁸⁶Sr is an important driver of bioavailable ⁸⁷Sr/⁸⁶Sr (Hoogewerff et al., 2019). The good performance of the bedrock model also reflects the high precision of geological maps used in the GLiM database for Europe (Hartmann and Moosdorf, 2012). Random forest regression using exclusively local bioavailable ⁸⁷Sr/⁸⁶Sr data is the model that best predicts bioavailable ⁸⁷Sr/⁸⁶Sr from the GEMAS dataset (Fig. 10D). However, the performance of this locally calibrated model is comparable to the globally calibrated models (Fig. 10B and 10C).

When calibrating a random forest using only GEMAS soil data, nitrogen fertilization rate becomes a significant predictor in the regression (Fig. 10D). As GEMAS is exclusively focused on agricultural soils, it is expected that fertilization practices (e.g., liming) impact ⁸⁷Sr/⁸⁶Sr in the exchangeable soil fraction (Frei et al., 2020; Hoogewerff et al., 2019; Thomsen and Andreasen, 2019). This predictor was not selected when calibrating the model using the combined global and local bioavailable ⁸⁷Sr/⁸⁶Sr dataset, which suggests that local calibration might be more appropriate in certain cases when trying to predict one specific substrate (e.g., soil). However, use of local calibrations that include more regionally- or system-specific model relationships caries the potential risk of producing errant predictions if the model is applied to areas where these relationships are irrelevant or inconsistent with the calibration data. A firm understanding of the underlying mechanisms and drivers of ⁸⁷Sr/⁸⁶Sr variation is crucial in developing and using such models.

We further demonstrate that the global random forest regression excluding GEMAS data (Fig. 10B) performs nearly as well as the random forest that includes GEMAS data (Fig. 10C). This observation highlights the potential of extrapolating predictions in data-rich regions. Importantly, we underline that removing the GEMAS dataset from the training set does not remove all the European data. Many studies have collected bioavailable ⁸⁷Sr/⁸⁶Sr data in Western Europe (see compilation in Bataille et al., 2018). While those datasets do not cover parts of eastern and northern Europe included in the GEMAS dataset, they do provide a strong basis for calibrating the relationships between bioavailable ⁸⁷Sr/⁸⁶Sr and the covariates in unsampled regions across the entire European continent. The success of this extrapolation

likely depends on the similarity of geological and environmental conditions found in the under-sampled areas with those of the training set. This observation also indicates that the sampling density in Europe is probably sufficient to train accurate ⁸⁷Sr/⁸⁶Sr isoscapes with the current set of predictors. Additional sampling will only improve this performance marginally.

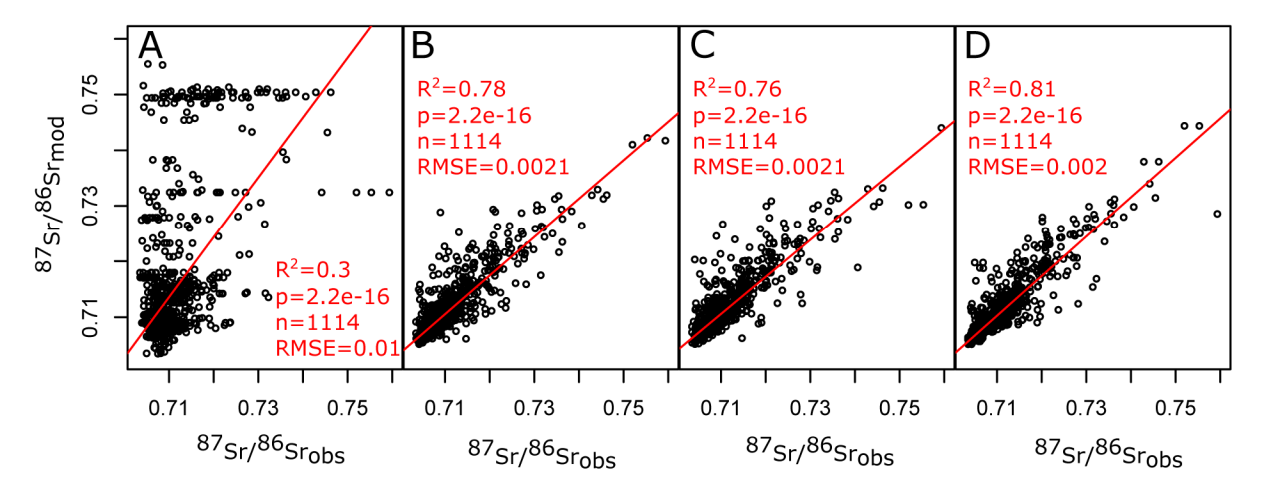


Figure 10: Cross-validation of different models for the GEMAS dataset: A) Bedrock model; B) Random forest regression calibrated using the global bioavailable data without data from GEMAS, C) Random forest regression calibrated using global bioavailable data including bioavailable data from GEMAS, and D) Random forest regression calibrated using bioavailable data from GEMAS only. Red lines are best-fit linear models.

5.3.2 Madagascar

In Madagascar, we found that the bedrock model does not perform as well as in Europe (Fig. 11A). This was not surprising as the map used in the GLiM for Madagascar is outdated and has a low resolution (Besairie, 1964). As mentioned earlier, Madagascar is a very geologically complex region, and the lack of detailed geological maps strongly limits the ability of the bedrock model to predict ⁸⁷Sr/⁸⁶Sr in the geosphere or the biosphere. A much more detailed geologic map of Madagascar does exist (Roig et al. 2012); integrating updated products like this into the GLiM will help improve global ⁸⁷Sr/⁸⁶Sr isoscape models.

In Madagascar, the performance of the locally calibrated model (Fig. 11D) is significantly improved in comparison with the globally calibrated models (Fig. 11B and 11C). Additionally, the globally calibrated model excluding Madagascar data performs poorly (Fig. 11B). While most of the bioavailable ⁸⁷Sr/⁸⁶Sr data fall on a strong correlation line, several large residuals limit the model accuracy. These large residuals are from bioavailable ⁸⁷Sr/⁸⁶Sr data collected on old metamorphic and sedimentary rock units that represent geological and/or environmental conditions that were not encountered in the combined local bioavailable ⁸⁷Sr/⁸⁶Sr training dataset. Under such conditions, extrapolation of global ⁸⁷Sr/⁸⁶Sr predictions becomes invalid. Even when including the Madagascar data in the global compilation, these data are not sufficient to fully overcome the strong predictive bias towards data-rich regions. This result underlines the need for local bioavailable ⁸⁷Sr/⁸⁶Sr data in regions that are geologically complex and under-sampled. With the current set of covariates, the global isoscape is well-calibrated for Europe and North America where most bioavailable ⁸⁷Sr/⁸⁶Sr data have been sampled but poorly calibrated in other regions. To solve this issue, more bioavailable ⁸⁷Sr/⁸⁶Sr data are required across Madagascar and Africa, particularly from

older radiogenic units, in order to calibrate the bioavailable ⁸⁷Sr/⁸⁶Sr model with geological and environmental predictors in this region.

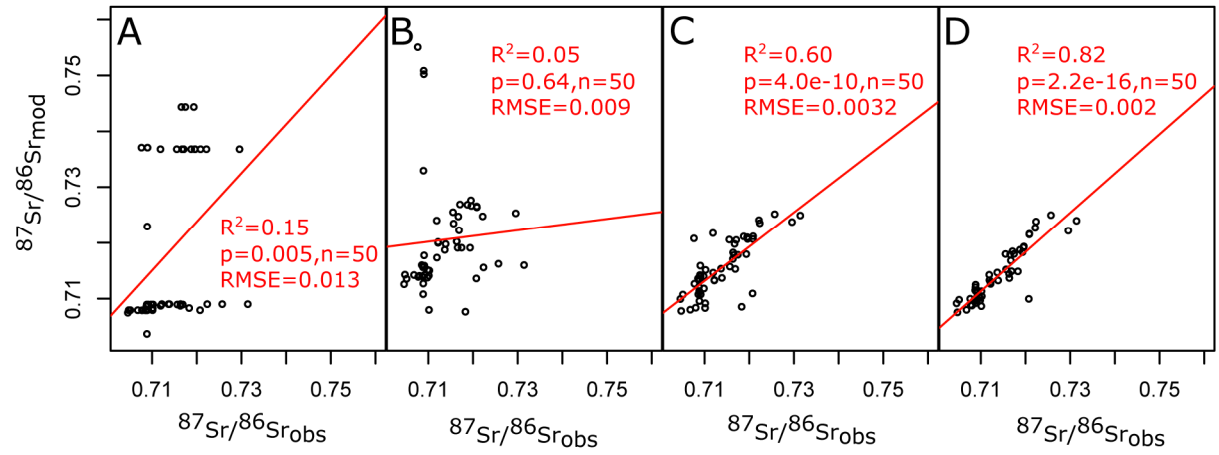


Figure 11: n-fold cross-validation of different models on the Madagascar dataset: A) Bedrock model; B) Random forest regression calibrated using the global bioavailable data without data from Madagascar, C) Random forest regression calibrated using global bioavailable data including bioavailable data from Madagascar, and D) Random forest regression calibrated using bioavailable data from Madagascar only. Red lines are best-fit linear models.

6. Guidelines, knowledge gaps and new research avenues

6.1 Guidelines for using the global isoscape

776

777

778

779780

781

782

783

784

785

786

787

788

789

790

791

792

793

794 795

796

797 798

799

800

801

802

803

804

805

806

807

808

809

810

811

Provenance studies have underlying assumptions specific to the sample type and the question being addressed. The predicted bioavailable ⁸⁷Sr/⁸⁶Sr isoscape presented here (Fig. 9) is best suited as a broad scale approach for 1) excluding provenance areas and 2) informing where targeted sampling for a specific research question should occur. When samples in question exhibit a limited range in bioavailable 87Sr/86Sr, as is the case for plants, soils, and animals with small feeding ranges (e.g., non-migratory rodents), the bioavailable ⁸⁷Sr/⁸⁶Sr isoscape can also be used to predict areas of natal origin. However, the current bioavailable ⁸⁷Sr/⁸⁶Sr isoscape can be considered robust only in data-rich areas, and extrapolations to other regions should be approached cautiously, particularly where geological and environmental conditions differ from those represented in the training set. In data-poor regions, the accuracy and resolution of the bioavailable ⁸⁷Sr/⁸⁶Sr isoscape should be tested by collecting additional data. We encourage other researchers to test, and if required recalibrate, their own ⁸⁷Sr/⁸⁶Sr isoscapes using the global framework presented here (see supplementary material script S1), and also to add new local bioavailable ⁸⁷Sr/⁸⁶Sr data to the global compilation (more details provided below). The number of additional data required to calibrate the model to a specific study area is challenging to determine. A cost-effective strategy would be to collect an initial small dataset to test the accuracy of the global bioavailable ⁸⁷Sr/⁸⁶Sr model to help verify its performance. When performance is poor (e.g., Madagascar), collecting more data should be considered depending on the scale of the study, the complexity of the geology and the existing distribution of bioavailable ⁸⁷Sr/⁸⁶Sr data. However, as additional data are included in the modeling, model predictions will probably degrade in some data-rich regions as the global model looks for the best prediction compromise given available data and covariates. The number of predictors will need to be increased to avoid this biasing. As demonstrated in this review, another possible solution for local and regional studies is to calibrate a model using only local to regional bioavailable ⁸⁷Sr/⁸⁶Sr data.

6.2 Knowledge gaps

6.2.1 Improving the global database, analytical methods, sampling strategy and centralized repository

812

813

814

815

816 817

818

819

820

821

822

823

824

825

826

827

828

829 830

831

832

833

834

835 836

837

838

839

840

841 842

843

844

845

846

847

848

849

850

851

852

853

854 855

856

857

858

859

860

Although the ⁸⁷Sr/⁸⁶Sr data used in the combined local bioavailable ⁸⁷Sr/⁸⁶Sr training dataset appear to be quite dense (Fig. 1), there are still huge data gaps in many environmental, geographic and geological settings that limit the accuracy of the global bioavailable ⁸⁷Sr/⁸⁶Sr isoscape. The current global compilation is heavily biased towards agricultural and densely populated regions of Europe and North America (Fig. 2). This sampling bias is propagated to the global ⁸⁷Sr/⁸⁶Sr isoscape, leading to degradation of predictions in under-sampled parts of the world (e.g., Madagascar). High latitudes, desert, semi-arid regions, tropics, wetlands, and mountainous areas are largely under-represented. Most cratonic regions and their associated sedimentary basins are also largely underrepresented (e.g., Africa, Australia, Canada, or Brazil). Gaps from many remote regions could be filled through targeted Sr isotope analysis of samples from museum collections (e.g., rodents; https://arctosdb.org/; Fig. 12). These samples could be used to facilitate the development of ⁸⁷Sr/⁸⁶Sr isoscapes in high-latitude regions with applications for migratory birds, megafauna or early human mobility. As demonstrated in this review, regional accuracy of the global model could be significantly improved by adding only tens to hundreds of points in under-sampled areas (Fig. 11). Conversely doubling the number of points in already well-sampled regions will only bring minor improvement (e.g., Europe). As bioavailable ⁸⁷Sr/⁸⁶Sr data are positively skewed, sampling needs to account for the higher variability in older and more complex geological settings. Sampling those regions at high density might help capture some of the high variance observed in these regions. This type of sampling rationale can be systematized using available statistical algorithms (e.g., Latin Hypercube) that use the distribution of existing covariates (e.g., geology, climate) to optimize the sampling strategy at a given location or globally (Minasny and McBratney, 2006).

Filling these data gaps will require ⁸⁷Sr/⁸⁶Sr analysis of thousands of samples. Despite significant analytical improvements in the last decades, analyzing ⁸⁷Sr/⁸⁶Sr is currently expensive and slow in comparison with other isotopic systems analyzed using continuous flow stable isotope ratio mass-spectrometry or cavity ring down spectroscopy. In the last few years, new methods have emerged that make ⁸⁷Sr/⁸⁶Sr analysis faster and more affordable, increasing the possibilities of generating high-density datasets. For example, the use of Laser Ablation (LA)-MC-ICPMS instead of solution methods for analyzing solid samples with high Sr content (e.g., animal teeth) allows very high throughput, limited sample preparation and sufficient analytical precision for most provenance studies (±0.0001). This method could help develop large datasets from museum specimens (e.g., rodents) and improve the accuracy of bioavailable ⁸⁷Sr/⁸⁶Sr isoscapes in remote regions (Fig. 12). More recently, the use of ICP-MS/MS with in-line Rb separation has been proposed to increase throughput, decrease cost and limit sample amount for solution methods (Murphy et al., 2020). This method provides fast and relatively inexpensive analysis of small biological samples (e.g., insect tissues) with similar analytical precision to LA-MC-ICPMS (±0.0001). Lastly, the addition of an autosampler with syringe injection on MC-ICP-MS instruments (e.g., microFAST-MC) has contributed to increased throughput and reduced mass requirements without compromising analytical precision. To increase throughput, MC-ICP-MS users could further reduce the integration time and number of ratios analyzed. This would decrease analytical precision, but, as mentioned above, precision of ± 0.0001 is usually sufficient in provenance studies. We encourage researchers to further develop and adopt these analytical methods to continue decreasing the price and time required for ⁸⁷Sr/⁸⁶Sr analysis.

One final critical issue when generating a bioavailable ⁸⁷Sr/⁸⁶Sr dataset is the lack of guidance on the metadata required when collecting bioavailable ⁸⁷Sr/⁸⁶Sr data (Grimstead et

al., 2017). Most bioavailable ⁸⁷Sr/⁸⁶Sr datasets include some fields representing location and isotopic data. The remaining metadata provided by authors vary as no metadata template exists in the community. This is problematic because different fields or substrates require different types of metadata. Moreover, many metadata fields are often required to better screen and use bioavailable ⁸⁷Sr/⁸⁶Sr data for provenance applications. In compiling the dataset for this study, geographic coordinates, substrate type (e.g., plant, soil, water, animal tissue), sample details (e.g., plant species, soil depth), tissue sampled (e.g., enamel versus dentine, whole plant versus leaves), analytical method,and analytical precision needed to be mined from the main manuscript or directly from the authors in many cases. This is time-consuming, not always successful, and could be entirely avoided if appropriate data and metadata templates were provided to the community. These challenges are being addressed by the development of IsoBank, a centralized repository for isotope data (Pauli et al., 2017). This repository will contain data templates specific for bioavailable ⁸⁷Sr/⁸⁶Sr data that will facilitate the integration of data from multiple sources and fields (planned launch date is 2021).

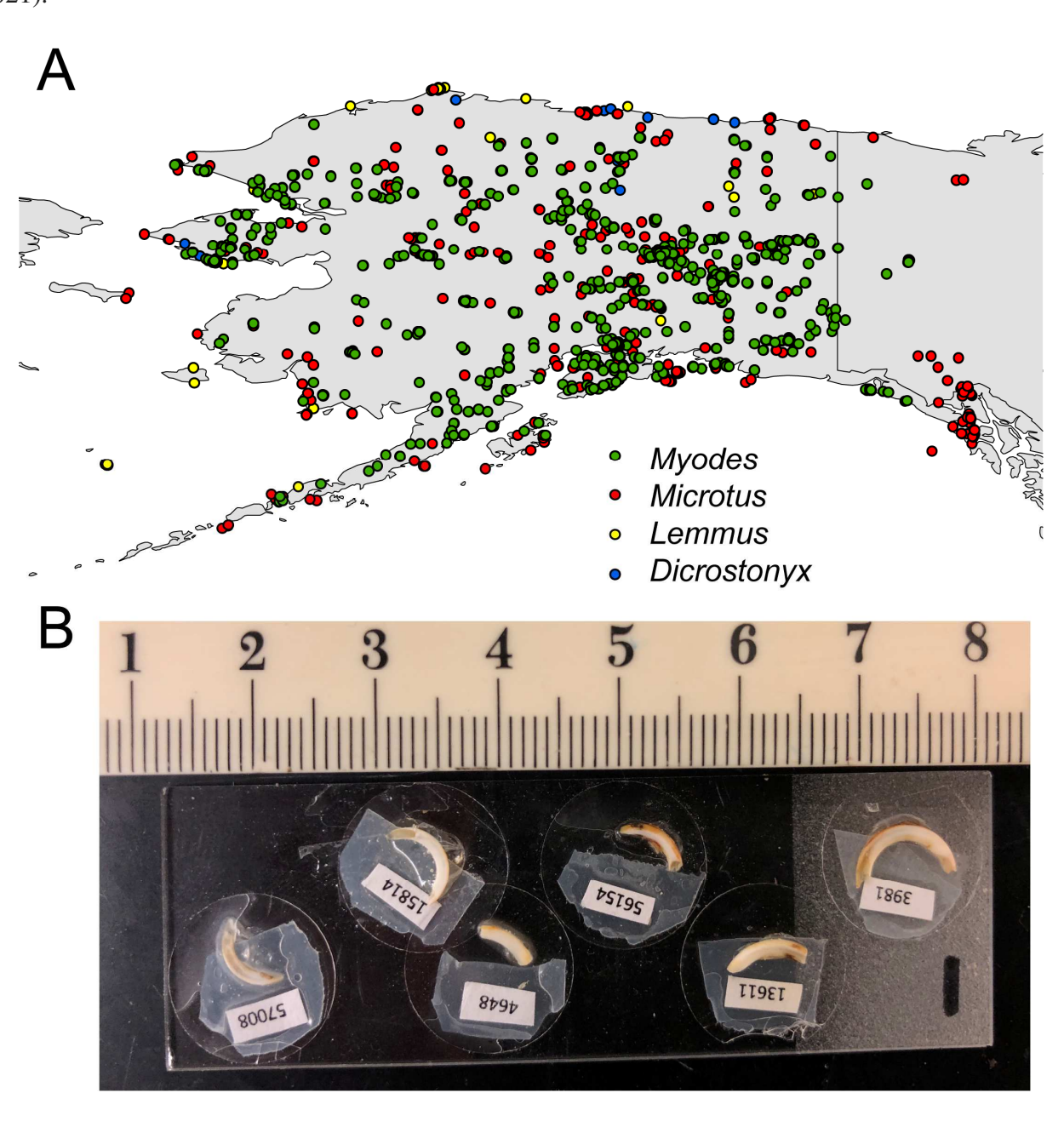


 Figure 12: An example of filling ⁸⁷Sr/⁸⁶Sr data gaps in a remote region (Alaska): A) Results of a query on the Arctos database (https://arctosdb.org/; Accessed April 1, 2020) for teeth of selected non-migratory rodents (including *Lemmus*, *Microtus*, *Myodes* and *Discrostonyx* species) in the mammal collection at the University of Alaska Museum of the North. B) Mounting of rodent teeth prepared for cost-effective and rapid LA-ICP-MS ⁸⁷Sr/⁸⁶Sr analysis.

6.2.2 Improving modeling

It has already been demonstrated that random forest outperforms most linear and non-linear models by better representing complex non-linear relationships in bioavailable ⁸⁷Sr/⁸⁶Sr data (Bataille et al., 2018). The current script (see supplementary material script S1) is designed to handle large datasets with dozens of covariates. This script uses parallelization to boost raster calculation and random forest prediction through the *caret* (Kuhn, 2008) and *doParallel* packages (Calaway et al., 2018). However, as the database of bioavailable ⁸⁷Sr/⁸⁶Sr data grows and/or more covariates are accounted for, the regression matrices will exceed the capability of desktop computers. This high computational intensity is one of the drawbacks of using random forest regression as the computational loads grow exponentially with more data. Random forest is also sensitive to noise and errors in the data and requires a careful quality check, which is often an issue with large interdisciplinary compilations.

As demonstrated in this review, the extrapolation of models fitted using random forest is suitable for data-rich regions but risky for data-poor regions with geologies that fall outside of the calibration dataset, or have outdated geology maps in the GLiM. Sampling biases are also propagated into the bioavailable ⁸⁷Sr/⁸⁶Sr predictions. Once enough bioavailable data are available from all parts of the world, one solution to limit biasing and computing time will be to train a model on a geographically well-distributed subset of the database. Many of the relationships found by random forest regression are also non-deterministic and not stationary. A good example of this issue is represented by the relationship between bioavailable ⁸⁷Sr/⁸⁶Sr and dust deposition (Fig. 8). In the global model, dust deposition combines information about dust flux and dust sources into one single variable (r.dust). If new bioavailable data are collected in regions with elevated dust flux with low ⁸⁷Sr/⁸⁶Sr (e.g., China), this will likely degrade the relationship between bioavailable ⁸⁷Sr/⁸⁶Sr and dust in the model. This type of issue underlines the need for additional and better covariates which would open-up more targeted modeling opportunities. A large part of the model uncertainty is due to the limitation of global geological maps. Including geological map products is currently essential, as they are the dominant predictors of bioavailable ⁸⁷Sr/⁸⁶Sr variability. However, their inaccuracies, lack of homogeneity in resolution and classification scheme, and boundary issues, are also transmitted to the predicted bioavailable ⁸⁷Sr/⁸⁶Sr variations. A continuous geospatial dataset that captures geological variability (e.g., radiometric data) or multispectral satellite data (e.g., WorldView-3) would considerably improve the situation. Lastly, while random forest can train accurate models, expert knowledge on geology, geochemistry and environmental science remain critical for interpreting model results. Calibrating a bioavailable ⁸⁷Sr/⁸⁶Sr isoscape requires carefully verifying the relationships between predictors and response variables. Ultimately random forest regression models should pave the way to improve mechanistic modeling approaches.

6.3 Conclusions and perspectives

Here we have presented the first validated, high-resolution ⁸⁷Sr/⁸⁶Sr isoscape at the global scale, which should be useful to many researchers interested in provenance applications. These ⁸⁷Sr/⁸⁶Sr isoscapes provide powerful templates for extrapolating between and beyond

the bounds of existing databases. They can be used independently or coupled with other isotopic systems (e.g., hydrogen, oxygen, and carbon) to provide provenance assignments in a range of fields. To date, ⁸⁷Sr/⁸⁶Sr has been largely underused in ecological applications in comparison with other isotopic systems. However, with the rapid advances in the development of ⁸⁷Sr/⁸⁶Sr isoscapes, we anticipate that ⁸⁷Sr/⁸⁶Sr will become a tool of choice for investigating the mobility of migratory species at large spatial scales. ⁸⁷Sr/⁸⁶Sr exhibits limited temporal variability but high-resolution spatial patterns, and offers unique advantages relative to other isotopic systems. New applications of ⁸⁷Sr/⁸⁶Sr to assess the population dynamics and migratory pathways of bird and insect species are ongoing and will reveal the potential of ⁸⁷Sr/⁸⁶Sr in this type of ecological applications. The global bioavailable ⁸⁷Sr/⁸⁶Sr isoscape is also relevant to investigations of the ecology of extinct animal species. Global ⁸⁷Sr/⁸⁶Sr paleo-isoscapes will be key to resolving questions about megafaunal ecology, early human dispersals, or human societies. Advances in ⁸⁷Sr/⁸⁶Sr isoscapes should also make this geochemical tracer increasingly relevant in forensic and food sciences. Such applications will probably require calibrating substrate-specific global ⁸⁷Sr/⁸⁶Sr baselines (e.g., drugs, wine). The up-front cost might be challenging, but once developed, these calibrated isoscapes will be valid for the long term and readily applicable to other markers. While considerable gaps remain in the development of global 87Sr/86Sr isoscape, this study paves the way for rapid advances in the applications of this tracer in large-scale provenance applications.

For researchers interested in biogeochemical cycles, the development of global ⁸⁷Sr/⁸⁶Sr isoscapes and ⁸⁷Sr/⁸⁶Sr compilations offers a novel and exciting research avenue for improving global Earth systems models. We have already underlined that developing pure mechanistic isoscapes is beyond our current knowledge of Sr isotope cycling. However, these knowledge gaps point to a key opportunity for advancing our understanding of biogeochemical cycles through ⁸⁷Sr/⁸⁶Sr modeling. It has long been known that ⁸⁷Sr/⁸⁶Sr is a unique tracer of elemental cycling in rivers, aerosols, and ecosystems at the local scale. Global predictive ⁸⁷Sr/⁸⁶Sr modeling provides the opportunity to scale up this tracer from the local to the global scale. For example, bioavailable ⁸⁷Sr/⁸⁶Sr modeling could provide a novel method for understanding soil weathering processes, or estimating the elemental contribution of aerosol inputs to ecosystems, while constraints gained from regression models could help advance the quantitative theory describing the controls of elemental cycling in the hydrosphere, atmosphere and ecosphere. Similarly, developing global ⁸⁷Sr/⁸⁶Sr isoscapes in river water would be relevant to better partitioning solute sources in watersheds. At the global scale, ⁸⁷Sr/⁸⁶Sr isoscapes could help quantify the global elemental flux from continental surfaces refining thereby global elemental budget in seawater. With the advances of plate models and paleogeological reconstructions, it might even be possible in the future to reconstruct ⁸⁷Sr/⁸⁶Sr on the Earth' surface in deep time to provide new constraints on global biogeochemical cycles in specific time periods.

Acknowledgments

923

924

925

926

927

928

929

930

931

932

933

934

935

936

937

938

939

940

941

942

943

944

945

946

947

948

949

950

951

952

953954

955

956

957

958

959

960

961

962

963 964

965

966

967

This work was supported in part by NSERC Discovery Grant RGPIN-2019-05709 (to C.P.B). This paper is dedicated to the memory of Dr. Sean Brennan who sadly passed away in January 2020. Dr. Brennan was a stellar young scientist, and had considerably advanced the Sr isoscape field. His work and his passion will be dearly missed. We thank Tom Johnson and Gideon Bartov for analyzing specimens at the University of Illinois Urbana-Champaign, and Steve Goodman, Lisa Kelly, Tim Eppley, and Mitch Irwin for assistance with sample

- ollection in Madagascar. B.E.C was supported by the UC faculty startup. G.J.B was
- 969 supported by NSF DBI-1759730. We thank Drs. Mandy Keogh, Brian Taras, Mark Nelson,
- and Lori Quakenbush from the Alaska Dept. of Fish & Game (ADF&G) for sharing the
- 971 ⁸⁷Sr/⁸⁶Sr data from Cook Inlet, which was funded by a NOAA ESA Section 6 grant to
- 972 ADF&G (NA17NMF4720071) with matching financial support provided by Georgia
- 973 Aquarium, SeaWorld & Busch Gard's Conservation Fund, and John G. Shedd Aquarium
- 974 (awarded to MK, MJW, LQ, MN and BT). We also thank: The Cook Inlet Keepers, Tyonek
- 975 Tribal Conservation District, Dr. Katrin Iken (UAF), Dr. Tamara McGuire (LGL), Tom Gage
- 976 (ADF&G), Justin Jenniges (ADF&G), Amber Stephens (LGL), Parker Bradley (ADF&G),
- 977 Ted Otis (ADF&G), Tom Cappiello, Sue Mauger, Chris Garner (DOD, JBER), Dr. Dan
- 978 Rinella (USFWS), and Dr. Paul Wade (NOAA) for collecting water samples and Dr. Diego
- 979 Fernandez and Christopher Anderson at the University of Utah for Sr analyses. We thank
- 980 Bernhard Peucker-Ehrenbrink and an anonymous reviewer for their constructive reviews.

981 References

- 982 Aarons, S.M., Aciego, S.M., Arendt, C.A., Blakowski, M.A., Steigmeyer, A., Gabrielli, P.,
- 983 Sierra-Hernández, M.R., Beaudon, E., Delmonte, B., Baccolo, G., May, N.W., Pratt,
- 984 K.A., 2017. Dust composition changes from Taylor Glacier (East Antarctica) during the
- last glacial-interglacial transition: A multi-proxy approach. Quat. Sci. Rev. 162, 60–71.
- 986 https://doi.org/10.1016/j.quascirev.2017.03.011
- Åberg, G., 1995. The use of natural strontium isotopes as tracers in environmental studies.
- 988 Water, Air, Soil Pollut. 79, 309–322. https://doi.org/10.1007/BF01100444
- Bain, D.C., Bacon, J.R., 1994. Strontium isotopes as indicators of mineral weathering in catchments. Catena 22, 201–214. https://doi.org/10.1016/0341-8162(94)90002-7
- 991 Balmino, G., Vales, N., Bonvalot, S., Briais, A., 2012. Spherical harmonic modelling to ultra-
- high degree of Bouguer and isostatic anomalies. J. Geod. 86, 499–520.
- 993 https://doi.org/10.1007/s00190-011-0533-4
- Banner, J.L., 2004. Radiogenic isotopes: Systematics and applications to earth surface
- processes and chemical stratigraphy. Earth-Science Rev. 65, 141–194.
- 996 https://doi.org/10.1016/S0012-8252(03)00086-2
- 997 Bartelink, E.J., Chesson, L.A., 2019. Recent applications of isotope analysis to forensic
- anthropology. Forensic Sci. Res. 4, 29–44.
- 999 https://doi.org/10.1080/20961790.2018.1549527
- Bataille, C.P., Bowen, G.J., 2012. Mapping ⁸⁷Sr/⁸⁶Sr variations in bedrock and water for large
- scale provenance studies. Chem. Geol. 304–305, 39–52.
- https://doi.org/10.1016/j.chemgeo.2012.01.028
- Bataille, C.P., Brennan, S.R., Hartmann, J., Moosdorf, N., Wooller, M.J., Bowen, G.J., 2014.
- A geostatistical framework for predicting variability in strontium concentrations and
- isotope ratios in Alaskan rivers. Chem. Geol. 389, 1–15.
- 1006 https://doi.org/10.1016/j.chemgeo.2014.08.030
- Bataille, C.P., von Holstein, I.C.C., Laffoon, J.E., Willmes, M., Liu, X.M., Davies, G.R.,
- 2018. A bioavailable strontium isoscape for Western Europe: A machine learning
- approach. PLoS One 13. https://doi.org/10.1371/journal.pone.0197386
- Beard, B.L., Johnson, C.M., 2000. Strontium Isotope Composition of Skeletal Material Can

- Determine the Birth Place and Geographic Mobility of Humans and Animals. J. Forensic
- 1012 Sci. 45, 1049–1061. https://doi.org/10.1520/JFS14829J
- Bentley, R.A., 2006. Strontium isotopes from the earth to the archaeological skeleton: A
- review. J. Archaeol. Method Theory 13, 135–187. https://doi.org/10.1007/s10816-006-
- 1015 9009-x
- Bern, C.R., Townsend, A.R., Farmer, G.L., 2005. Unexpected dominance of parent-material
- strontium in a tropical forest on highly weathered soils. Ecology 86, 626–632.
- 1018 https://doi.org/10.1890/03-0766
- 1019 Besairie, H., 1964. Carte Géologique de Madagascar. Antananarivo.
- Bickle, M.J., Chapman, H.J., Tipper, E., Galy, A., De La Rocha, C.L., Ahmad, T., 2018.
- 1021 Chemical weathering outputs from the flood plain of the Ganga. Geochim. Cosmochim.
- 1022 Acta 225, 146–175. https://doi.org/10.1016/j.gca.2018.01.003
- Bickle, M.J., Harris, N.B.W., Bunbury, J.M., Chapman, H.J., Fairchild, I.J., Ahmad, T., 2001.
- 1024 Controls on the ⁸⁷Sr/⁸⁶Sr ratio of carbonates in the Garhwal Himalaya, Headwaters of the
- 1025 Ganges. J. Geol. 109, 737–753. https://doi.org/10.1086/323192
- Bickle, M.J., Wickham, S.M., Chapman, H.J., Taylor, H.P., 1988. A strontium, neodymium
- and oxygen isotope study of hydrothermal metamorphism and crustal anatexis in the
- Trois Seigneurs Massif, Pyrenees, France. Contrib. to Mineral. Petrol. 100, 399–417.
- 1029 https://doi.org/10.1007/BF00371371
- Blum, J.D., Erel, Y., Brown, K., 1993. 87Sr/86Sr ratios of sierra nevada stream waters:
- 1031 Implications for relative mineral weathering rates. Geochim. Cosmochim. Acta 57,
- 1032 5019–5025. https://doi.org/10.1016/S0016-7037(05)80014-6
- Blum, J.D., Taliaferro, E.H., Weisse, M.T., Holmes, R.T., 2000. Changes in Sr/Ca, Ba/Ca
- and ⁸⁷Sr/⁸⁶Sr ratios between trophic levels in two forest ecosystems in the northeastern
- 1035 U.S.A. Biogeochemistry 49, 87–101. https://doi.org/10.1023/A:1006390707989
- Börker, J., Hartmann, J., Amann, T., Romero-Mujalli, G., 2018. Terrestrial sediments of the
- earth: Development of a global unconsolidated sediments map database (gum).
- Geochemistry, Geophys. Geosystems 19, 997–1024.
- 1039 https://doi.org/10.1002/2017GC007273
- Bowen, G.J., Liu, Z., Vander Zanden, H.B., Zhao, L., Takahashi, G., 2014. Geographic
- assignment with stable isotopes in IsoMAP. Methods Ecol. Evol. 5, 201–206.
- 1042 https://doi.org/10.1111/2041-210X.12147
- Bowen, G.J., West, J.B., 2008. Isotope Landscapes for Terrestrial Migration Research. Terr.
- Ecol. 2, 79–105. https://doi.org/10.1016/S1936-7961(07)00004-8
- Bowen, G.J., Wilkinson, B., 2002. Spatial distribution of δ^{18} O in meteoric precipitation.
- Geology 30, 315–318. https://doi.org/10.1130/0091-7613(2002)030<0315
- Brennan, S.R., Fernandez, D.P., Zimmerman, C.E., Cerling, T.E., Brown, R.J., Wooller, M.J.,
- 2015a. Strontium isotopes in otoliths of a non-migratory fish (slimy sculpin):
- 1049 Implications for provenance studies. Geochim. Cosmochim. Acta 149, 32–45.
- 1050 https://doi.org/10.1016/j.gca.2014.10.032
- Brennan, S.R., Schindler, D.E., Cline, T.J., Walsworth, T.E., Buck, G., Fernandez, D.P.,
- 2019. Shifting habitat mosaics and fish production across river basins. Science (80-.).

- 1053 364, 783–786. https://doi.org/10.1126/science.aav4313
- Brennan, S.R., Zimmerman, C.E., Fernandez, D.P., Cerling, T.E., McPhee, M. V., Wooller,
- M.J., 2015b. Strontium isotopes delineate fine-scale natal origins and migration histories
- of Pacific salmon. Sci. Adv. 1, e1400124–e1400124.
- 1057 https://doi.org/10.1126/sciadv.1400124
- Burney, D.A., Andriamialison, H., Andrianaivoarivelo, R.A., Bourne, S., Crowley, B.E., De
- Boer, E.J., Godfrey, L.R., Goodman, S.M., Griffiths, C., Griffiths, O., Hume, J.P.,
- Joyce, W.G., Jungers, W.L., Marciniak, S., Middleton, G.J., Muldoon, K.M.,
- Noromalala, E., Pérez, V.R., Perry, G.H., Randalana, R., Wright, H.T., 2020. Subfossil
- lemur discoveries from the Beanka Protected Area in western Madagascar. Quat. Res.
- 1063 (United States) 93, 187–203. https://doi.org/10.1017/qua.2019.54
- Burton, J.H., Price, T.D., 2013. Seeking the local ⁸⁷Sr/⁸⁶Sr ratio to determine geographic
- origins of humans, in: ACS Symposium Series. https://doi.org/10.1021/bk-2013-
- 1066 1147.ch018
- 1067 Calaway, R., Weston, S., Tenenbaum, D., 2018. Package 'doParallel.' CRAN Repos.
- Capo, R.C., Stewart, B.W., Chadwick, O.A., 1998. Strontium isotopes as tracers of
- ecosystem processes: theory and methods. Geoderma 82, 197–225.
- 1070 Chadwick, O.A., Derry, L.A., Bern, C.R., Vitousek, P.M., 2009. Changing sources of
- strontium to soils and ecosystems across the Hawaiian Islands. Chem. Geol. 267, 64–76.
- https://doi.org/10.1016/j.chemgeo.2009.01.009
- 1073 Chamberlain, C.P., Blum, J.D., Holmes, R.T., Sherry, T.W., Graves, G.R., 1997. The use of
- isotope tracers for identifying populations of migratory birds. Oecologia 109, 132–141.
- 1075 Clow, D.W., Mast, M.A., Bullen, T.D., Turk, J.T., 1997. Strontium ⁸⁷/strontium ⁸⁶ as a tracer
- of mineral weathering reactions and calcium sources in an alpine/subalpine watershed,
- Loch Vale, Colorado. Water Resour. Res. 33, 1335–1351.
- 1078 https://doi.org/10.1029/97WR00856
- 1079 Coelho, I., Castanheira, I., Bordado, J.M., Donard, O., Silva, J.A.L., 2017. Recent
- developments and trends in the application of strontium and its isotopes in biological
- related fields. TrAC Trends Anal. Chem. 90, 45–61.
- 1082 https://doi.org/10.1016/j.trac.2017.02.005
- Copeland, S.R., Cawthra, H.C., Fisher, E.C., Lee-Thorp, J.A., Cowling, R.M., le Roux, P.J.,
- Hodgkins, J., Marean, C.W., 2016. Strontium isotope investigation of ungulate
- movement patterns on the Pleistocene Paleo-Agulhas Plain of the Greater Cape Floristic
- 1086 Region, South Africa. Quat. Sci. Rev. 141, 65–84.
- 1087 https://doi.org/10.1016/j.quascirev.2016.04.002
- 1088 Copeland, S.R., Sponheimer, M., De Ruiter, D.J., Lee-Thorp, J.A., Codron, D., Le Roux, P.J.,
- Grimes, V., Richards, M.P., 2011. Strontium isotope evidence for landscape use by early
- hominins. Nature 474, 76–78. https://doi.org/10.1038/nature10149
- 1091 Crowley, B.E., Castro, I., Soarimalala, V., Goodman, S.M., 2018. Isotopic evidence for niche
- partitioning and the influence of anthropogenic disturbance on endemic and introduced
- rodents in central Madagascar. Sci. Nat. 105, 44. https://doi.org/10.1007/s00114-018-
- 1094 1564-y
- 1095 Crowley, B.E., Godfrey, L.R., 2019. Strontium Isotopes Support Small Home Ranges for

- Extinct Lemurs. Front. Ecol. Evol. 7, 490. https://doi.org/10.3389/fevo.2019.00490
- 1097 Crowley, B.E., Miller, J.H., Bataille, C.P., 2017a. Strontium isotopes (87Sr/86Sr) in terrestrial
- ecological and palaeoecological research: empirical efforts and recent advances in
- continental-scale models. Biol. Rev. 92, 43–59. https://doi.org/10.1111/brv.12217
- 1100 Crowley, B.E., Slater, P.A., Arrigo-Nelson, S.J., Baden, A.L., Karpanty, S.M., 2017b.
- Strontium isotopes are consistent with low-elevation foraging limits for Henst's
- goshawk. Wildl. Soc. Bull. 41, 743–751. https://doi.org/10.1002/wsb.840
- 1103 Curtis, J.B., Stueber, A.M., 1973. ⁸⁷Sr/⁸⁶Sr ratios and total strontium concentrations in surface waters of the Scioto River drainage basin, Ohio. Ohio J. Sci. 73, 166–175.
- Douglas, T.A., Blum, J.D., Guo, L., Keller, K., Gleason, J.D., 2013. Hydrogeochemistry of
- seasonal flow regimes in the Chena River, a subarctic watershed draining discontinuous
- permafrost in interior Alaska (USA). Chem. Geol. 335, 48–62.
- https://doi.org/10.1016/j.chemgeo.2012.10.045
- Evans, J.A., Montgomery, J., Wildman, G., Boulton, N., 2010. Spatial variations in biosphere
- 1110 87Sr/86Sr in Britain. J. Geol. Soc. London. 167, 1–4. https://doi.org/10.1144/0016-
- 1111 76492009-090
- Ezzo, J.A., Johnson, C.M., Price, T.D., 1997. Analytical perspectives on prehistoric
- migration: A case study from East-Central Arizona. J. Archaeol. Sci. 24, 447–466.
- https://doi.org/10.1006/jasc.1996.0129
- Faure, G., Crocket, J.H., Hueley, P.M., 1967. Some aspects of the geochemistry of strontium
- and calcium in the Hudson Bay and the Great Lakes. Geochim. Cosmochim. Acta 31,
- 451–461. https://doi.org/10.1016/0016-7037(67)90053-1
- Faure, G., Powell, J.L., 1972. Strontium Isotope Geology, Strontium Isotope Geology.
- Springer-Verlag Berlin, Heidelberg, New York, USA. https://doi.org/10.1007/978-3-
- 1120 642-65367-4
- 1121 Feranec, R.S., Hadly, E.A., Paytan, A., 2007. Determining landscape use of Holocene
- mammals using strontium isotopes. Oecologia 153, 943–950.
- https://doi.org/10.1007/s00442-007-0779-y
- Flockhart, D.T.T.T., Kyser, T.K., Chipley, D., Miller, N.G., Norris, D.R., 2015. Experimental
- evidence shows no fractionation of strontium isotopes (87Sr/86Sr) among soil, plants, and
- herbivores: implications for tracking wildlife and forensic science. Isotopes Environ.
- Health Stud. 51, 372–381. https://doi.org/10.1080/10256016.2015.1021345
- Frei, K.M., Frei, R., 2011. The geographic distribution of strontium isotopes in Danish
- surface waters A base for provenance studies in archaeology, hydrology and
- agriculture. Appl. Geochemistry 26, 326–340.
- https://doi.org/10.1016/j.apgeochem.2010.12.006
- Frei, R., Frei, K.M., Jessen, S., 2020. Shallow retardation of the strontium isotope signal of
- agricultural liming implications for isoscapes used in provenance studies. Sci. Total
- Environ. 706, 135710. https://doi.org/10.1016/J.SCITOTENV.2019.135710
- 1135 Frumkin, A., Stein, M., 2004. The Sahara-East Mediterranean dust and climate connection
- revealed by strontium and uranium isotopes in a Jerusalem speleothem. Earth Planet.
- 1137 Sci. Lett. 217, 451–464. https://doi.org/10.1016/S0012-821X(03)00589-2

- Galy, A., France-Lanord, C., 1999. The strontium isotopic budget of Himalayan rivers in Nepal and Bangladesh. Geochim. Cosmochim. Acta 63, 1905–1925.
- 1140 Genuer, R., Poggi, J.-M., Tuleau-Malot, C., 2015. VSURF: An R Package for Variable
- Selection Using Random Forests. R J. 7, 19–33.
- https://doi.org/10.1016/j.cell.2007.09.012
- Glassburn, C.L., Potter, B.A., Clark, J.L., Reuther, J.D., Bruning, D.L., Wooller, M.J., 2018.
- Strontium and oxygen isotope profiles of sequentially sampled modern bison (Bison
- bison bison) teeth from interior alaska as proxies of seasonal mobility. Arctic 71, 183–
- 200. https://doi.org/10.14430/arctic4718
- Glorennec, P., Lucas, J.-P., Mercat, A.-C., Roudot, A.-C., Le Bot, B., 2016. Environmental
- and dietary exposure of young children to inorganic trace elements. Environ. Int. 97, 28–
- 36. https://doi.org/10.1016/J.ENVINT.2016.10.009
- Good, S.P., Noone, D., Bowen, G., 2015. Hydrologic connectivity constrains partitioning of
- global terrestrial water fluxes. Science (80-.). 349, 175–177.
- https://doi.org/10.1126/science.aaa5931
- Gosz, J.R., Brookins, D.G., Moore, D.I., 1983. Using Strontium Isotope Ratios to Estimate
- Inputs to Ecosystems. Bioscience 33, 23–30. https://doi.org/10.2307/1309240
- Grimstead, D.N., Nugent, S., Whipple, J., 2017. Why a Standardization of Strontium Isotope
- Baseline Environmental Data Is Needed and Recommendations for Methodology. Adv.
- 1157 Archaeol. Pract. 5, 184–195. https://doi.org/10.1017/aap.2017.6
- Grousset, F.E., Biscaye, P.E., Revel, M., Petit, J.R., Pye, K., Joussaume, S., Jouzel, J., 1992.
- Antarctic (Dome C) ice-core dust at 18 k.y. B.P.: Isotopic constraints on origins. Earth
- Planet. Sci. Lett. 111, 175–182. https://doi.org/10.1016/0012-821X(92)90177-W
- Gryschko, R., Kuhnle, R., Terytze, K., Breuer, J., Stahr, K., 2005. Soil extraction of readily
- soluble heavy metals and as with 1 M NH4NO3-solution. Evaluation of DIN 19730. J.
- Soils Sediments 5, 101–106. https://doi.org/10.1065/jss2004.10.119
- Hamilton, M., Nelson, S. V., Fernandez, D.P., Hunt, K.D., 2019. Detecting riparian habitat
- preferences in "savanna" chimpanzees and associated Fauna with strontium isotope
- ratios: Implications for reconstructing habitat use by the chimpanzee-human last
- 1167 common ancestor. Am. J. Phys. Anthropol. 170, 551–564.
- 1168 https://doi.org/10.1002/ajpa.23932
- Hartman, G., Richards, M., 2014. Mapping and defining sources of variability in bioavailable
- strontium isotope ratios in the Eastern Mediterranean. Geochim. Cosmochim. Acta 126,
- 250–264. https://doi.org/10.1016/j.gca.2013.11.015
- Hartmann, J., Moosdorf, N., 2012. The new global lithological map database GLiM: A
- representation of rock properties at the Earth surface. Geochemistry, Geophys.
- Geosystems 13. https://doi.org/10.1029/2012GC004370
- Hedman, K.M., Curry, B.B., Johnson, T.M., Fullagar, P.D., Emerson, T.E., 2009. Variation
- in strontium isotope ratios of archaeological fauna in the Midwestern United States: a
- preliminary study. J. Archaeol. Sci. 36, 64–73. https://doi.org/10.1016/j.jas.2008.07.009
- Hegg, J.C., Kennedy, B.P., Fremier, A.K., 2013. Predicting strontium isotope variation and
- fish location with bedrock geology: Understanding the effects of geologic heterogeneity.
- 1180 Chem. Geol. 360–361, 89–98. https://doi.org/10.1016/j.chemgeo.2013.10.010

- Hengl, T., Mendes de Jesus, J., Heuvelink, G.B.M., Ruiperez Gonzalez, M., Kilibarda, M.,
- Blagotić, A., Shangguan, W., Wright, M.N., Geng, X., Bauer-Marschallinger, B.,
- Guevara, M.A., Vargas, R., MacMillan, R.A., Batjes, N.H., Leenaars, J.G.B., Ribeiro,
- E., Wheeler, I., Mantel, S., Kempen, B., 2017. SoilGrids250m: Global gridded soil
- information based on machine learning. PLoS One 12, e0169748.
- https://doi.org/10.1371/journal.pone.0169748
- Hijmans, R.J., Cameron, S.E., Parra, J.L., Jones, P.G., Jarvis, A., 2005. Very high resolution
- interpolated climate surfaces for global land areas. Int. J. Climatol. 25, 1965–1978.
- 1189 https://doi.org/10.1002/joc.1276
- Hobson, K.A., Barnett-Johnson, R., Cerling, T., 2010. Using isoscapes to track animal
- migration, in: Isoscapes: Understanding Movement, Pattern, and Process on Earth
- through Isotope Mapping. Springer Netherlands, Dordrecht, pp. 273–298.
- https://doi.org/10.1007/978-90-481-3354-3_13
- Hoogewerff, J.A., Reimann, Clemens, Ueckermann, H., Frei, R., Frei, K.M., van Aswegen,
- T., Stirling, C., Reid, M., Clayton, A., Ladenberger, A., Albanese, S., Andersson, M.,
- Baritz, R., Batista, M.J., Bel-lan, A., Birke, M., Cicchella, D., Demetriades, A., De
- Vivo, B., De Vos, W., Dinelli, E., Ďuriš, M., Dusza-Dobek, A., Eggen, O.A., Eklund,
- M., Ernstsen, V., Filzmoser, P., Flight, D.M., Forrester, S., Fuchs, M., Fügedi, U.,
- Gilucis, A., Gregorauskiene, V., De Groot, W., Gulan, A., Halamić, J., Haslinger, E.,
- Hayoz, P., Hoffmann, R., Hrvatovic, H., Husnjak, S., Janik, L., Jordan, G., Kaminari,
- M., Kirby, J., Kivisilla, J., Klos, V., Krone, F., Kwećko, F., Kuti, L., Lima, A., Locutura,
- J., Lucivjansky, D., Mann, A., Mackovych, D., Matschullat, J., McLaughlin, M.,
- Malyuk, B., Maquil, R., Meuli, R.G., Mol, G., Negrel, P., Connor, O., Oorts, R.,
- Ottesen, R.T., Pasieczna, A., Petersell, W., Pfleiderer, S., Poňavič, M., Pramuka, S.,
- Prazeres, C., Rauch, U., Radusinović, S., Reimann, C., Sadeghi, M., Salpeteur, I.,
- Scanlon, R., Schedl, A., Scheib, A., Schoeters, I., Šefčik, P., Sellersjö, E., Skopljak, F.,
- Slaninka, I., Soriano-Disla, J.M., Šorša, A., Srvkota, R., Stafilov, T., Tarvainen, T.,
- Trendavilov, V., Valera, P., Verougstraete, V., Vidojević, D., Zissimos, A., Zomeni, Z.,
- 2019. Bioavailable ⁸⁷Sr/⁸⁶Sr in European soils: A baseline for provenancing studies. Sci.
- Total Environ. 672, 1033–1044. https://doi.org/10.1016/J.SCITOTENV.2019.03.387
- Hoppe, K.A., Koch, P.L., Carlson, R.W., Webb, S.D., 1999. Tracking mammoths and
- mastodons: Reconstruction of migratory behavior using strontium isotope ratios.
- 1213 Geology 27, 439–442. https://doi.org/10.1130/0091-
- 1214 7613(1999)027<0439:TMAMRO>2.3.CO;2
- Jarvis, A., H.I., Reuter, A., Nelson, A., Guevara, E., 2008. Hole-filled SRTM for the globe
- 1216 Version 4, available from the CGIAR-CSI SRTM 90m Database. CGIAR CSI Consort.
- Spat. Inf. 1–9. https://doi.org/http://srtm.csi.cgiar.org
- Kennedy, B.P., Blum, J.D., Folt, C.L., Nislow, K.H., 2000. Using natural strontium isotopic
- signatures as fish markers: methodology and application. Can. J. Fish. Aquat. Sci. 57,
- 1220 2280–2292. https://doi.org/10.1139/f00-206
- Kennedy, B.P., Klaue, A., Blum, J.D., Folt, C.L., Nislow, K.H., 2002. Reconstructing the
- lives of fish using Sr isotopes in otoliths. Can. J. Fish. Aquat. Sci. 59, 925–929.
- 1223 https://doi.org/10.1139/f02-070
- Koch, P.L., Heisinger, J., Moss, C., Carlson, R.W., Fogel, M.L., Behrensmeyer, A.K., 1995a.
- 1225 Isotopic tracking of change in diet and habitat use in African elephants. Science (80-.).

- 267, 1340–1343. https://doi.org/10.1126/science.267.5202.1340
- Koch, P.L., Zachos, J.C., Dettman, D.L., 1995b. Stable isotope stratigraphy and
- paleoclimatology of the Paleogene Bighorn Basin (Wyoming, USA). Palaeogeogr.
- Palaeoclimatol. Palaeoecol. 115, 61–89. https://doi.org/10.1016/0031-0182(94)00107-J
- 1230 Kramer, R.T., Bartelink, E.J., Herrmann, N.P., Bataille, C.P., Spradley, K., 2020. Application
- of stable isotopes and geostatistics to infer region of geographical origin for deceased
- undocumented Latin American migrants, in: Forensic Science and Humanitarian Action.
- 1233 https://doi.org/10.1002/9781119482062.ch27
- Kuhn, M., 2008. Building Predictive Models in R Using the caret Package. J. Stat. Softw. 28,
- 1235 1–26. https://doi.org/10.1053/j.sodo.2009.03.002
- Laffoon, J.E., Davies, G.R., Hoogland, M.L.P., Hofman, C.L., 2012. Spatial variation of
- biologically available strontium isotopes (87Sr/86Sr) in an archipelagic setting: A case
- study from the Caribbean. J. Archaeol. Sci. 39, 2371–2384.
- 1239 https://doi.org/10.1016/j.jas.2012.02.002
- Lengfelder, F., Grupe, G., Stallauer, A., Huth, R., Söllner, F., 2019. Modelling strontium
- isotopes in past biospheres Assessment of bioavailable ⁸⁷Sr/⁸⁶Sr ratios in local
- archaeological vertebrates based on environmental signatures. Sci. Total Environ. 648,
- 1243 236–252. https://doi.org/10.1016/j.scitotenv.2018.08.014
- Lewis, J., Pike, A.W.G., Coath, C.D., Evershed, R.P., 2017. Strontium concentration,
- radiogenic (87 Sr/ 86 Sr and stable (88 Sr) strontium isotope systematics in a controlled
- feeding study. Sci. Technol. Archaeol. Res. 3, 45–57.
- 1247 https://doi.org/10.1080/20548923.2017.1303124
- Lupker, M., France-Lanord, C., Galy, V., Lavé, J., Gaillardet, J., Gajurel, A.P., Guilmette, C.,
- Rahman, M., Singh, S.K., Sinha, R., 2012. Predominant floodplain over mountain
- weathering of Himalayan sediments (Ganga basin). Geochim. Cosmochim. Acta 84,
- 1251 410–432. https://doi.org/10.1016/j.gca.2012.02.001
- Mahowald, N.M., Muhs, D.R., Levis, S., Rasch, P.J., Yoshioka, M., Zender, C.S., Luo, C.,
- 1253 2006. Change in atmospheric mineral aerosols in response to climate: Last glacial
- period, preindustrial, modern, and doubled carbon dioxide climates. J. Geophys. Res.
- 1255 Atmos. 111. https://doi.org/10.1029/2005JD006653
- Makarewicz, C.A., Sealy, J., 2015. Dietary reconstruction, mobility, and the analysis of
- ancient skeletal tissues: Expanding the prospects of stable isotope research in
- archaeology. J. Archaeol. Sci. 56, 146–158. https://doi.org/10.1016/j.jas.2015.02.035
- Maurer, A.F., Galer, S.J.G., Knipper, C., Beierlein, L., Nunn, E. V., Peters, D., Tütken, T.,
- Alt, K.W., Schöne, B.R., 2012. Bioavailable ⁸⁷Sr/⁸⁶Sr in different environmental
- samples Effects of anthropogenic contamination and implications for isoscapes in past
- migration studies. Sci. Total Environ. 433, 216–229.
- 1263 https://doi.org/10.1016/j.scitotenv.2012.06.046
- McArthur, J.M., Howarth, R.J., Bailey, T.R., 2001. Strontium isotope stratigraphy: LOWESS
- version 3: Best fit to the marine Sr-isotope curve for 0-509 Ma and accompanying look-
- up table for deriving numerical age. J. Geol. 109, 155–170.
- 1267 https://doi.org/10.1086/319243
- Miller, O.L., Solomon, D.K., Fernandez, D.P., Cerling, T.E., Bowling, D.R., 2014.

- Evaluating the use of strontium isotopes in tree rings to record the isotopic signal of dust
- deposited on the Wasatch Mountains. Appl. Geochemistry 50, 53–65.
- 1271 https://doi.org/10.1016/j.apgeochem.2014.08.004
- Minasny, B., McBratney, A.B., 2006. A conditioned Latin hypercube method for sampling in
- the presence of ancillary information. Comput. Geosci. 32, 1378–1388.
- 1274 https://doi.org/10.1016/j.cageo.2005.12.009
- Mooney, W.D., Laske, G., Masters, T.G., 1998. CRUST 5.1: A global crustal model at $5^{\circ} \times$
- 5°. J. Geophys. Res. Solid Earth 103, 727–747. https://doi.org/10.1029/97JB02122
- Murphy, D.T., Allen, C.M., Ghidan, O., Dickson, A., Hu, W.P., Briggs, E., Holder, P.W.,
- Armstrong, K.F., 2020. Analysing Sr isotopes in low-Sr samples such as single insects
- with inductively coupled plasma tandem mass spectrometry using N_2O as a reaction gas
- for in-line Rb separation. Rapid Commun. Mass Spectrom. 15, e8604.
- 1281 https://doi.org/10.1002/rcm.8604
- Naiman, Z., Quade, J., Patchett, P.J., 2000. Isotopic evidence for eolian recycling of
- pedogenic carbonate and variations in carbonate dust sources throughout the southwest
- 1284 United States. Geochim. Cosmochim. Acta 64, 3099–3109.
- https://doi.org/10.1016/S0016-7037(00)00410-5
- Nier, A.O., 1938. The isotopic constitution of Strontium, Barium, Bismuth, Thallium and Mercury. Phys. Rev. 54. https://doi.org/10.1103/PhysRev.54.275
- 1288 Palmer, M.R., Edmond, J.M., 1992. Controls over the strontium isotope composition of river
- water. Geochim. Cosmochim. Acta 56, 2099–2111. https://doi.org/10.1016/0016-
- 1290 7037(92)90332-D
- Pauli, J.N., Newsome, S.D., Cook, J.A., Harrod, C., Steffan, S.A., Baker, C.J.O., Ben-David,
- M., Bloom, D., Bowen, G.J., Cerling, T.E., Cicero, C., Cook, C., Dohm, M., Dharampal,
- P.S., Graves, G., Gropp, R., Hobson, K.A., Jordan, C., MacFadden, B., Pilaar Birch, S.,
- Poelen, J., Ratnasingham, S., Russell, L., Stricker, C.A., Uhen, M.D., Yarnes, C.T.,
- Hayden, B., 2017. Opinion: Why we need a centralized repository for isotopic data.
- Proc. Natl. Acad. Sci. 114, 2997–3001. https://doi.org/10.1073/pnas.1701742114
- Pett-Ridge, J.C., Derry, L.A., Kurtz, A.C., 2009. Sr isotopes as a tracer of weathering
- processes and dust inputs in a tropical granitoid watershed, Luquillo Mountains, Puerto
- Rico. Geochim. Cosmochim. Acta 73, 25–43. https://doi.org/10.1016/j.gca.2008.09.032
- Peucker-Ehrenbrink, B., Fiske, G.J., 2019. A continental perspective of the seawater ⁸⁷Sr/⁸⁶Sr
- record: A review. Chem. Geol. 510, 140–165.
- https://doi.org/10.1016/j.chemgeo.2019.01.017
- Porder, S., Clark, D.A., Vitousek, P.M., 2006. Persistence of rock-derived nutrients in the wet
- tropical forests of La Selva, Costa Rica. Ecology 87, 594–602.
- 1305 https://doi.org/10.1890/05-0394
- Poszwa, A., Ferry, B., Dambrine, E., Pollier, B., Wickman, T., Loubet, M., Bishop, K., 2004.
- Variations of bioavailable Sr concentration and ⁸⁷Sr/⁸⁶Sr ratio in boreal forest
- ecosystems: Role of biocycling, mineral weathering and depth of root uptake.
- Biogeochemistry 67, 1–20. https://doi.org/10.1023/B:BIOG.0000015162.12857.3e
- Potter, P., Ramankutty, N., Bennett, E.M., Donner, S.D., 2010. Characterizing the spatial
- patterns of global fertilizer application and manure production. Earth Interact. 14, 1–22.

- 1312 https://doi.org/10.1175/2009EI288.1
- 1313 Price, G.J., Ferguson, K.J., Webb, G.E., Feng, Y.X., Higgins, P., Nguyen, A.D., Zhao, J.X.,
- Joannes-Boyau, R., Louys, J., 2017. Seasonal migration of marsupial megafauna in
- pleistocene sahul (Australia-New Guinea). Proc. R. Soc. B Biol. Sci. 284.
- 1316 https://doi.org/10.1098/rspb.2017.0785
- Price, T.D., Johnson, C.M., Ezzo, J.A., Ericson, J., Burton, J.H., 1994. Residential mobility in
- the prehistoric southwest United States: A preliminary study using strontium isotope
- analysis. J. Archaeol. Sci. 21, 315–330. https://doi.org/10.1006/jasc.1994.1031
- Quade, J., Chivas, A.R., McCulloch, M.T., 1995. Strontium and carbon isotope tracers and
- the origins of soil carbonate in South Australia and Victoria. Palaeogeogr.
- Palaeoclimatol. Palaeoecol. 113, 103–117. https://doi.org/10.1016/0031-0182(95)00065-
- 1323 T
- Reynolds, A.C., Quade, J., Betancourt, J.L., 2012. Strontium isotopes and nutrient sourcing in
- a semi-arid woodland. Geoderma 189–190, 574–584.
- https://doi.org/10.1016/j.geoderma.2012.06.029
- Schulting, R., Richards, M., Pouncett, J., Manco, B.N., Freid, E., Ostapkowicz, J., 2018.
- Absence of Saharan dust influence on the strontium isotope ratios on modern trees from
- the Bahamas and Turks and Caicos Islands. Quat. Res. (United States) 89, 394–412.
- 1330 https://doi.org/10.1017/qua.2018.8
- Sillen, A., Hall, G., Richardson, S., Armstrong, R., 1998. 87Sr/86Sr ratios in modern and fossil
- food-webs of the Sterkfontein Valley: Implications for early hominid habitat preference.
- 1333 Geochim. Cosmochim. Acta 62, 2463–2473. https://doi.org/10.1016/S0016-
- 1334 7037(98)00182-3
- Snoeck, C., Schulting, R.J., Lee-Thorp, J.A., Lebon, M., Zazzo, A., 2016. Impact of heating
- conditions on the carbon and oxygen isotope composition of calcined bone. J. Archaeol.
- 1337 Sci. 65, 32–43. https://doi.org/10.1016/j.jas.2015.10.013
- Steiger, R.H., Jäger, E., 1977. Subcommission on geochronology: Convention on the use of
- decay constants in geo- and cosmochronology. Earth Planet. Sci. Lett. 36, 359–362.
- https://doi.org/10.1016/0012-821X(77)90060-7
- Still, C.J., Powell, R.L., 2010. Continental-scale distributions of vegetation stable carbon
- isotope ratios, in: Isoscapes: Understanding Movement, Pattern, and Process on Earth
- through Isotope Mapping. Springer Netherlands, Dordrecht, pp. 179–193.
- https://doi.org/10.1007/978-90-481-3354-3_9
- 1345 Strobl, C., Boulesteix, A.L., Zeileis, A., Hothorn, T., 2007. Bias in random forest variable
- importance measures: Illustrations, sources and a solution. BMC Bioinformatics 8, 25.
- 1347 https://doi.org/10.1186/1471-2105-8-25
- Thomsen, E., Andreasen, R., 2019. Agricultural lime disturbs natural strontium isotope
- variations: Implications for provenance and migration studies. Sci. Adv. 5, eaav8083.
- 1350 https://doi.org/10.1126/sciadv.aav8083
- Thorrold, S.R., Shuttleworth, S., 2000. In situ analysis of trace elements and isotope ratios in
- fish otoliths using laser ablation sector field inductively coupled plasma mass
- spectrometry. Can. J. Fish. Aquat. Sci. 57, 1232–1242. https://doi.org/10.1139/f00-054
- Vautour, G., Poirier, A., Widory, D., 2015. Tracking mobility using human hair: What can

- we learn from lead and strontium isotopes? Sci. Justice 55, 63–71.
- 1356 https://doi.org/10.1016/j.scijus.2014.10.001
- 1357 Vet, R., Artz, R.S., Carou, S., Shaw, M., Ro, C.U., Aas, W., Baker, A., Bowersox, V.C.,
- Dentener, F., Galy-Lacaux, C., Hou, A., Pienaar, J.J., Gillett, R., Forti, M.C., Gromov,
- S., Hara, H., Khodzher, T., Mahowald, N.M., Nickovic, S., Rao, P.S.P., Reid, N.W.,
- 2014. A global assessment of precipitation chemistry and deposition of sulfur, nitrogen,
- sea salt, base cations, organic acids, acidity and pH, and phosphorus. Atmos. Environ.
- 93, 3–100. https://doi.org/10.1016/j.atmosenv.2013.10.060
- Vitousek, P.M., Kennedy, M.J., Derry, L.A., Chadwick, O.A., 1999. Weathering versus
- atmospheric sources of strontium in ecosystems on young volcanic soils. Oecologia 121,
- 1365 255–259. https://doi.org/10.1007/s004420050927
- Voerkelius, S., Lorenz, G.D., Rummel, S., Quétel, C.R., Heiss, G., Baxter, M., Brach-Papa,
- 1367 C., Deters-Itzelsberger, P., Hoelzl, S., Hoogewerff, J., Ponzevera, E., Van Bocxstaele,
- M., Ueckermann, H., 2010. Strontium isotopic signatures of natural mineral waters, the
- reference to a simple geological map and its potential for authentication of food. Food
- 1370 Chem. 118, 933–940. https://doi.org/10.1016/j.foodchem.2009.04.125
- Voss, B.M., Peucker-Ehrenbrink, B., Eglinton, T.I., Fiske, G., Wang, Z.A., Hoering, K.A.,
- Montluçon, D.B., LeCroy, C., Pal, S., Marsh, S., Gillies, S.L., Janmaat, A., Bennett, M.,
- Downey, B., Fanslau, J., Fraser, H., Macklam-Harron, G., Martinec, M., Wiebe, B.,
- 1374 2014. Tracing river chemistry in space and time: Dissolved inorganic constituents of the
- 1375 Fraser River, Canada. Geochim. Cosmochim. Acta 124, 283–308.
- https://doi.org/10.1016/j.gca.2013.09.006
- Walker, J.D., Geissman, J.W., Bowring, S.A., Babcock, L.E., 2018. Geologic Time Scale.
- 1378 Geol. Soc. Am. https://doi.org/10.1130/2018
- Wallace, J.P., Crowley, B.E., Miller, J.H., 2019. Investigating equid mobility in Miocene
- Florida, USA using strontium isotope ratios. Palaeogeogr. Palaeoclimatol. Palaeoecol.
- 1381 516, 232–243. https://doi.org/10.1016/j.palaeo.2018.11.036
- West, J.B., Bowen, G.J., Dawson, T.E., Tu, K.P., 2010a. Isoscapes: Understanding
- movement, pattern, and process on earth through isotope mapping, Springer N. ed,
- 1384 Isoscapes: Understanding Movement, Pattern, and Process on Earth Through Isotope
- 1385 Mapping. Springer, Dordrecht. https://doi.org/10.1007/978-90-481-3354-3_14
- West, J.B., Bowen, G.J., Dawson, T.E., Tu, K.P., 2010b. Isoscapes: Understanding
- movement, pattern, and process on earth through isotope mapping, Isoscapes:
- Understanding Movement, Pattern, and Process on Earth Through Isotope Mapping.
- 1389 Springer Netherlands, Dordrecht. https://doi.org/10.1007/978-90-481-3354-3
- Wetherill, G.W., Mark, R., Lee-Hu, C., 1973. Chondrites: Initial strontium-87/strontium-86
- ratios and the early history of the solar system. Science (80-.). 182, 281–283.
- https://doi.org/10.1126/science.182.4109.281
- Whipkey, C.E., Capo, R.C., Chadwick, O.A., Stewart, B.W., 2000. The importance of sea
- spray to the cation budget of a coastal Hawaiian soil: A strontium isotope approach.
- 1395 Chem. Geol. 168, 37–48. https://doi.org/10.1016/S0009-2541(00)00187-X
- Widga, C., Walker, J.D., Boehm, A., 2017. Variability in Bioavailable ⁸⁷Sr/⁸⁶Sr in the North
- American Midcontinent. Open Quat. 3, 4. https://doi.org/10.5334/oq.32

1398 Widory, D., Liu, X., Dong, S., 2010. Isotopes as tracers of sources of lead and strontium in aerosols (TSP & PM2.5) in Beijing. Atmos. Environ. 44, 3679–3687. 1399 https://doi.org/10.1016/j.atmosenv.2010.06.036 1400 Willmes, M., Bataille, C.P., James, H.F., Moffat, I., McMorrow, L., Kinsley, L., Armstrong, 1401 R.A., Eggins, S., Grün, R., 2018. Mapping of bioavailable strontium isotope ratios in 1402 France for archaeological provenance studies. Appl. Geochemistry 90, 75–86. 1403 1404 https://doi.org/10.1016/j.apgeochem.2017.12.025 Willmes, M., Glessner, J.J.G., Carleton, S.A., Gerrity, P.C., Hobbs, J.A., 2016. 87Sr/86Sr 1405 isotope ratio analysis by laser ablation MC-ICP-MS in scales, spines, and fin rays as a 1406 nonlethal alternative to otoliths for reconstructing fish life history, Can. J. Fish. Aquat. 1407 Sci. 73, 1–9. https://doi.org/10.1139/cjfas-2016-0103 1408 1409 Willmes, M., McMorrow, L., Kinsley, L., Armstrong, R., Aubert, M., Eggins, S., Falguères, C., Maureille, B., Moffat, I., Grün, R., 2014. The IRHUM (Isotopic Reconstruction of 1410 Human Migration) database - Bioavailable strontium isotope ratios for geochemical 1411 fingerprinting in France. Earth Syst. Sci. Data 6, 117-122. https://doi.org/10.5194/essd-1412 6-117-2014 1413 Wunder, M.B., 2012. Determining geographic patterns of migration and dispersal using 1414 1415 stable isotopes in keratins. J. Mammal. 93, 360–367. https://doi.org/10.1644/11-MAMM-S-182.1 1416